Green Chemistry Meets Restorative Dentistry: Unlocking the Bioactive and Mineral Potential of Garden Cress (Lepidium sativum) Oil Through Gum Arabic-Mediated Delivery into Conventional Glass Ionomer Cement: An In-Vitro Appraisal

Neven Aref

n.aref@qu.edu.sa

College of Dentistry, Qassim University

Research Article

Keywords: Bioactive Potential, Garden Cress, GIC, Gum Arabic, Green Chemistry, Lepidium Sativum

Posted Date: August 5th, 2026

DOI: https://doi.org/10.21203/rs.3.rs-10486496/v1

Additional Declarations: No competing interests reported.

Green Chemistry Meets Restorative Dentistry: Unlocking the Bioactive and Mineral Potential of Garden Cress (Lepidium sativum) Oil Through Gum Arabic-Mediated Delivery into Conventional Glass Ionomer Cement: An *In-Vitro* Appraisal

Neven S. Aref,[1,2*]

[1]Department of Basic Oral Sciences and Dental Education, College of Dentistry, Qassim University, Buraydah, Saudi Arabia

[2]Department of Dental Biomaterials, Faculty of Dentistry, Mansoura University, Mansoura, Egypt

Type of manuscript: Research article

Short running title: Gum Arabic stabilization of GCO-modified GIC

Corresponding Author:

Name Neven Aref

Address College of Dentistry, Qassim University, Buraydah, Saudi Arabia

Phone number +201003978955/+966597500462

E-mail address n.aref@qu.edu.sa

ORCID: https://orcid.org/0000-0002-5241-2838

Abstract

Objectives: To evaluate the effect of incorporating Garden Cress (Lepidium sativum), fixed oil at three concentrations via Gum Arabic on the compressive strength, surface microhardness, surface roughness, and colour stability of conventional glass ionomer cement (GIC). **Materials and Methods:** Five groups (n = 10): G1 (unmodified control), G2 (GIC + 0.5 wt.% Gum Arabic), G3–G5 (GIC + Gum Arabic + 0.5, 1.0, 1.5 vol.% oil). Compressive strength, Vickers microhardness, surface roughness, and color difference (ΔE) against the control were measured alongside FTIR and SEM characterisation. One-way ANOVA with Tukey HSD was applied ($\alpha = 0.05$). **Results:** All outcomes showed significant group differences ($p < 0.0001$). G3 achieved the highest compressive strength (97.10 ± 3.75 MPa), exceeding the control (89.39 ± 3.13 MPa). G2 recorded the highest microhardness (73.33 ± 2.56 VHN) and smoothest surface (Ra = 0.488 ± 0.053 μm); G3 performed comparably at the surface level. Both properties declined progressively at 1.0 and 1.5 vol.%. Colour deviation increased dose-dependently; G2–G4 remained within the clinically acceptable range ($\Delta E < 3.3$), while G5 exceeded this threshold (4.01 ± 0.37). FTIR, SEM, and EDX findings provided chemical, morphological, and elemental corroboration of the mechanical and surface outcomes. **Conclusions:** Lepidium sativum fixed oil at 0.5 vol.% via Gum Arabic significantly enhanced compressive strength without compromising surface microhardness, surface smoothness, or colour acceptability. Higher concentrations produced progressive deterioration across all tested properties. 0.5 vol.% Lepidium sativum oil-modified formulation represents the optimal design *in-vitro*.

Clinical Significance: This 0.5 vol.% Lepidium sativum oil-modified formulation demonstrated superior mechanical performance and clinically acceptable aesthetic color deviation, suggesting potential as a bioactive-enhanced restorative cement for both esthetic and potential load-bearing applications.

Keywords: Bioactive Potential; Garden Cress; GIC; Gum Arabic; Green Chemistry; Lepidium Sativum

1. Introduction

Glass ionomer cement (GIC) has occupied a central and persistent position in restorative dentistry since its introduction by Wilson and Kent in 1972 [1]. The material's widespread clinical acceptance is attributable to a collection of properties that are unique among restorative

materials: the sustained, long-term release of fluoride ions capable of inhibiting secondary carious demineralization, direct chemical adhesion to enamel and dentine through ionic exchange with calcium in the hydroxyapatite lattice without the requirement for etching or bonding agents, a coefficient of thermal expansion closely matching that of tooth structure, and an inherent biocompatibility arising from the biological inertness of its mature glass-polysalt matrix [2, 3]. To address this drawback, high-viscosity (condensable or packable) GICs were introduced and became widely adopted for atraumatic restorative treatment (ART) during the early 1990s. These materials are formulated with finely milled glass particles, high-molecular-weight anhydrous polyacrylic acids, and an increased powder-to-liquid ratio, enabling faster setting, enhanced consistency, and improved handling characteristics. Although their physical formulation differs from that of conventional GICs, the hardening process remains governed by the same acid–base reaction mechanism. [4-6].

Despite these clinically significant advantages, conventional GIC carries well-documented limitations that restrict its application and compromise long-term clinical outcomes. The material's compressive strength, diametral tensile strength, and surface microhardness are substantially inferior to those of resin composite and resin-modified GIC, confining its use to low-stress clinical contexts and rendering it inappropriate for posterior load-bearing restorations in permanent dentitions [7-9]. Conventional GIC is inherently brittle, susceptible to surface crazing and microcracking under mechanical and thermal challenges, and particularly vulnerable to early moisture contamination during the aqueous setting phase — a window during which irreversible matrix disruption can occur [10,11]. Surface degradation under masticatory loading and oral challenge further compromises the clinical durability of GIC restorations, and secondary caries — the leading cause of restorative failure worldwide — continues to motivate the search for materials with improved surface integrity and mechanical durability [12].

The enhancement of conventional GIC to improve its mechanical and surface performance — specifically compressive strength, surface microhardness, surface smoothness, and colour stability — without compromising its fundamental clinical advantages of fluoride release and chemical adhesion, remains a central and unresolved challenge in contemporary dental biomaterials research [13,14]. Strategies investigated to date span a broad spectrum: reinforcement with inorganic fillers including hydroxyapatite nanoparticles, silica, and bioactive glass; incorporation of metallic nanoparticles including silver, zinc oxide, and titanium dioxide; addition of polymeric agents; and, increasingly, the incorporation of plant-

derived bioactive compounds including essential oils, phytochemical extracts, and fixed oils [15-20]. Among these, plant-derived bioactive oils have attracted particular investigative interest in recent years, predicated on their multifunctional biological profiles, their natural and renewable origin, their established safety in oral health applications, and — critically for a subset of compositionally mineral-rich oils — their potential to interact with the glass-polyacid matrix of GIC in a manner that may influence mechanical properties through mineral-mediated mechanisms [21].

The incorporation of essential and fixed oils into GIC matrices has been the subject of a growing number of *in vitro* investigations. Eugenol-rich clove oil was among the investigated, establishing that natural oil incorporation into GIC is technically feasible, with clear concentration-dependent mechanical effects at higher loadings [22]. Thyme oil and cinnamon oil have similarly been incorporated into GIC matrices, and could improve its antimicrobial efficacy and fluoride release without compromising compressive strength, with 5% cinnamon oil demonstrating the most favorable overall performance. [23]. The authors have previously reported the effects of fixed oil incorporation into conventional GIC, demonstrating that the mineral content of plant-derived oils — particularly calcium and phosphorus — provides a compositionally coherent basis for interaction with the glass phase and polyacid matrix, with documented beneficial effects on mechanical properties at low concentrations [15]. These collective findings have established plant-derived oils as a reasonable and productive opportunity for GIC modification research, whilst simultaneously revealing a consistent and critical methodological limitation that has not been adequately addressed in the existing literature.

A fundamental physicochemical incompatibility exists between hydrophobic plant-derived oils and the aqueous solutions. Direct oil addition without a structured carrier system into aqueous solutions produce phase separation and inhomogeneous distribution [24]. Oil modification of GIC can induce phase separation within the cement matrix, generating inconsistent and often deleterious mechanical outcomes. Accordingly, the absence of a reproducible carrier system to achieve homogeneous oil distribution within the GIC liquid prior to cement mixing represents the most significant unaddressed methodological gap in the oil-modified GIC literature.

Garden cress oil (GCO), the cold-pressed fixed oil extracted from the seeds of Lepidium sativum L. (family Brassicaceae), emerges as an exceptionally compelling and — to the authors' knowledge — entirely uninvestigated candidate for GIC modification. Lepidium sativum is an annual herb with a deep and extensively documented history in traditional

medicine across North Africa, the Arabian Peninsula, the Indian subcontinent, and the Mediterranean basin, where its seeds have been valued for centuries for their nutritive, wound-healing, diuretic, and anti-inflammatory properties. Additionally, it is proposed to have biological activities including antimicrobial, antidiabetic, antioxidant, antidiarrheal, anticancer, and numerous health-promoting effects in *in vivo* and *in vitro* studies [25]. Lepidium sativum seeds possess a complex phytochemical profile comprising proteins, lipids rich in oleic and linolenic acids, dietary fiber, essential minerals such as potassium, phosphorus, calcium, and iron, as well as diverse bioactive constituents. These include phytosterols (e.g., sitosterol, campesterol, and avenasterol), carotenoids, alkaloids, phenolic acids, glucosinolates, and antioxidant vitamins, including riboflavin, ascorbic acid, and tocopherols. The diversity of these constituents is believed to underlie the broad biological and therapeutic activities attributed to the plant. [26-28]. Of particular scientific relevance to GIC modification, Lepidium sativum seeds contain documented and substantial quantities of calcium, phosphorus, iron, magnesium, and zinc [29] — a mineral profile that provides a mechanistically coherent and directly analogous compositional rationale to that of sesame oil for GIC modification, supporting a hypothesis of mineral-mediated interaction with the fluoroaluminosilicate glass phase and the polyacrylic acid matrix of conventional GIC.

Critically, despite this extensive and well-established pharmacological characterization, Lepidium sativum oil has not been investigated in the context of any dental restorative material like conventional GIC — a verifiable, significant, and clinically relevant research gap.

To overcome the fundamental incompatibility between the hydrophobic garden cress oil and the aqueous GIC liquid phase, the present study employs Gum Arabic (GA) (acacia gum, E414) as a natural, biocompatible, and food-grade emulsifying carrier. Gum Arabic is a complex arabinogalactan polysaccharide-protein exudate obtained from the stems and branches of Acacia senegal (L.) Willd. and Acacia seyal Del., and is recognised as one of the most extensively characterised and widely utilised natural emulsifiers in pharmaceutical, food, and cosmetic industries [30,31]. Its capacity for oil-in-water emulsification derives from its unique amphiphilic molecular architecture, in which hydrophilic arabinogalactan polysaccharide chains are covalently linked to hydrophobic arabinogalactan-protein fractions; this structure enables rapid adsorption at the oil-water interface, formation of a viscoelastic interfacial protective film, and stabilization of oil droplets against coalescence and gravitational separation [32]. At the low concentration employed in the present study (0.5 wt.% of the GIC liquid phase), Gum Arabic is expected to provide adequate oil distribution capacity without

significantly altering the polyacrylic acid chemistry, the acid-base setting reaction, or the overall physicochemical properties of the cement — an expectation directly tested by the inclusion of a Gum Arabic-only control group (G2) in the experimental design. Gum Arabic has demonstrated negligible cytotoxicity and excellent biocompatibility in pharmaceutical and limited dental applications [33], supporting its suitability as a carrier material in a restorative cement context.

On the basis of the foregoing evidence, the present study was designed to test the hypothesis that incorporating Lepidium sativum fixed bioactive oil into conventional glass ionomer cement at 0.5, 1.0, and 1.5 vol.% using Gum Arabic as a natural carrier would produce significant, dose-dependent effects on compressive strength, surface microhardness, surface roughness, and color stability. The methodological hypothesis states that Gum Arabic at 0.5 wt.% would achieve adequate distribution of the oil within the GIC liquid, producing homogeneous oil incorporation at low concentrations which may be confirmed by scanning electron microscopy, and elemental analysis. The null hypothesis states that oil incorporation would produce no statistically significant differences in the compressive strength, surface microhardness, surface roughness, or color stability of conventional glass ionomer cement compared to the unmodified control. This investigation constitutes, to the authors' knowledge, the first report of Lepidium sativum oil incorporation into any dental restorative material, and the first application of a natural carrier system for fixed oil modification of conventional glass ionomer cement.

2. Materials and Methods

2.1 Study Design

This study was conducted as a controlled, comparative, *in vitro* experimental investigation. Five experimental groups were evaluated: an unmodified GIC control (G1), a Gum Arabic carrier-only control group without oil (G2), and three concentrations of Gum Arabic-stabilized garden cress oil-modified GIC (G3, G4, G5). The inclusion of G2 as an independent carrier control allows direct isolation of any effect attributable to Gum Arabic alone, independent of the garden cress oil. All specimens were fabricated, stored, and tested under standardized laboratory conditions (23 ± 1°C, 50 ± 5% relative humidity) throughout the duration of the study.

2.2 Experimental Design

2.2.1 Experimental Groups

Five experimental groups were designated as detailed in Table 1. The concentration of Gum Arabic was fixed at 0.5 wt.% of the total GIC liquid volume across all modified groups (G2–G5). Garden cress oil concentrations of 0.5, 1.0, and 1.5 vol.% were selected to span a biologically relevant and mechanically conservative range.

2.2.2 Sample Size Calculation

Sample size was determined a priori using G*Power software (version 3.1) for a one-way analysis of variance (ANOVA) design with five independent groups, using compressive strength as the primary outcome measure. Based on large effect sizes (Cohen's f = 0.60) reported in prior *in vitro* investigations of fixed oil incorporation into conventional glass ionomer cement [15], a significance level of $\alpha = 0.05$ (two-tailed), and a minimum desired statistical power of 80%, the required minimum sample size was calculated as n = 10 specimens per group (total N = 50 per test), yielding an achieved power of 91.6%. This sample size was therefore considered adequate and appropriate for the present investigation.

2.3 Materials

2.3.1 Glass Ionomer Cement

Conventional glass ionomer cement: Riva Self Cure (powder/liquid conventional glass ionomer restorative material; SDI Limited, Bayswater, Victoria 3153, Australia), high-viscosity encapsulated formulation. Mixed at the standard manufacturer-specified powder/liquid ratio. Lot number and expiry date recorded at time of use.

2.3.2 Garden Cress Oil

Cold-pressed fixed oil of Lepidium sativum L. seeds (Hemani Cress Seed Oil; manufactured by Hemani International KEPZ, Karachi, Pakistan; marketed by Hemani General Trading LLC, Dubai, UAE; under license from Hemani Herbal LLC, Longwood, FL, USA), characterized by FTIR prior to study commencement. Color: pale yellow. Stored at 4°C in sealed amber glass vials.

2.3.3 Gum Arabic

Gum Arabic (Acacia gum) powder (Jacquard®, Product No. JAC1648, Rupert, Gibbon & Spider, Inc., Healdsburg, CA, USA) was used as the natural emulsifying and stabilizing agent in this study.

2.4 Emulsion Preparation Protocol

All modifications were introduced exclusively to the GIC liquid phase. The GIC powder was used without alteration in all experimental groups.

Phase 1 — Preparation of Gum Arabic/GIC Liquid Stock

Gum Arabic powder of 0.03 g (0.5 wt.%) were dissolved in 0.6 mL of distilled water by magnetic stirring at 300 rpm until completely clear. The dissolved solution was combined with 6 mL of the GIC liquid to produce the Gum Arabic/GIC liquid stock, then stirred continuously at 300 rpm for a minimum of 24 hours prior to oil addition and specimen fabrication.

Phase 2 — Addition of Garden Cress Oil and Emulsification (G3, G4, G5)

Garden cress oil was added to the Gum Arabic/GIC liquid stock at 0.5 vol.% (G3), 1.0 vol.% (G4), and 1.5 vol.% (G5). A drop by drop oil addition was considered while mixtures were subjected to continuous magnetic stirring at 300 rpm for 24 hours. Emulsions were inspected visually immediately before specimen fabrication. Group G2 received no oil addition and was subjected to the same 24-hour stirring protocol.

Phase 3 — GIC Specimen Fabrication

Recommended powder and liquid ratio were mixed on a glass slab using a flexible stainless-steel spatula according to manufacturer instructions, transferred to lubricated split molds, condensed under a 1 kg weight for 10 minutes, then demolded, inspected, labelled, and stored individually in distilled water at 37 ± 1°C for 24 hours prior to testing, in accordance with ISO 9917-1:2007 requirements for compressive strength specimens and consistent with the standard protocol adopted in comparable *in vitro* GIC modification studies.

2.5 Outcome Measures and Testing Protocols

The following parameters were evaluated for the present analysis (Table 2). All mechanical and surface properties were assessed with the designed number of specimens per group.

2.5.1 FTIR Spectroscopy

FTIR spectra measurements were carried out for set specimens (n=3 representative per group) using a Bruker FT-IR spectrometer (Invenio S, Germany). The spectral resolution was 4 cm^{-1}, scans number was 64 and the wavenumber range of 400–4000 cm^{-1} was applied to the collection of IR spectra.

2.5.2 Scanning Electron Microscopy (SEM)

Scanning Electron Microscopy (JEOL, JSM- 6510LV, Japan) was performed on dedicated, intact, non-fractured disc specimens, prepared and polished. Specimens were gold-palladium sputter-coated and examined at 20 kV accelerating voltage at magnifications of ×2000, ×5000 ×10000.

2.5.3 Energy-Dispersive X-ray Analysis (EDX)

EDX elemental analysis was performed on the same specimens used for SEM, with particular attention to phosphorus (P) as a diagnostic marker of garden cress oil incorporation, alongside carbon (C), calcium (Ca), silicon (Si), aluminum (Al), and fluorine (F).

2.5.4 Compressive Strength

Cylindrical specimens (6 mm diameter × 4 mm height, n=10 per group) were fabricated per ISO 9917-1:2007. After 24-hour water storage at 37°C, specimens were tested using a universal testing machine (Lloyd Instruments Ltd., Fareham, UK) at a crosshead speed of 0.5 mm/min). Compressive strength (MPa) was calculated as

$$\mathbf{CS = 4F/(\pi d^2)}$$

, where F is the maximum load at fracture (N) and d is the specimen diameter (mm).

2.5.5 Surface Microhardness

Disc specimens (10 mm diameter × 2 mm height, n=10 per group) were wet-ground on 600-grit silicon carbide paper. Surface microhardness was measured by a Vickers microdurometer (Micromet II, Buehler, Lake Bluff, IL, USA) under a 200 gf load for 15 seconds; the mean of five indentations per specimen was recorded (VHN).

2.5.6 Surface Roughness

Surface roughness (Ra, μm) was measured on the disc specimens (n=10 per group) using a contact stylus profilometer (Mitutoyo, Sakado, Japan) (cut-off λc = 0.8 mm; evaluation length 4.0 mm). Three measurements per specimen were averaged.

2.5.7 Color Stability (ΔE)

Color stability was assessed on the same polished disc specimens (n = 10 per group). Color measurements were performed using a calibrated spectrophotometer (Vita Zahnfabrik H. Rauter GmbH & Co. KG, Bad Sackingen, Germany). Three measurements were recorded per specimen and averaged. The unmodified control (G1) was designated as the colour reference baseline, and the mean color difference (ΔE) between each modified group (G2–G5) and the control (G1) was calculated using the CIELAB colour space formula:

$$\Delta E = [(\Delta L^*)^2 + (\Delta a^*)^2 + (\Delta b^*)^2]^{1/2}$$

, where ΔL*, Δa*, and Δb* represent the differences in lightness, red-green, and yellow-blue coordinates between the modified and control specimens, respectively. A ΔE value of less than 3.3 was considered clinically acceptable, consistent with published perceptibility and acceptability thresholds for dental restorative materials.

2.6 Statistical Analysis

All quantitative data were analyzed using (SPSS, version 25; IBM Corp., Chicago, IL, USA). Normality was assessed using the Shapiro-Wilk test and homogeneity of variance using Levene's test. One-way analysis of variance (ANOVA) was applied to identify statistically significant differences among the five groups for each outcome variable. Post-hoc pairwise comparisons were performed using the Tukey Honestly Significant Difference (HSD) test, with exact critical values obtained from the studentized range distribution. Statistical significance was defined as $p < 0.05$. Data are presented as mean ± standard deviation. Groups sharing the same superscript letter were not significantly different at the 0.05 level.

3. Results

3.1 Fourier-Transform Infrared (FTIR) Spectroscopy

FTIR spectra were obtained for all five experimental groups across the wavenumber range of 400–4000 cm^{-1} (**Figure 1**). All five groups exhibited the principal absorption bands characteristic of conventional glass ionomer cement, including a broad O–H stretching band in the 3343–3396 cm^{-1} region, aliphatic C–H stretching at approximately 2922–2925 cm^{-1}, a carbonyl/carboxylate absorption region between 1581 and 1634 cm^{-1}, a C–H bending band at approximately 1455–1456 cm^{-1}, a carboxylate symmetric stretching band at 1402–1405 cm^{-1}, and a Si–O–Si/C–O band at 1024–1038 cm^{-1} attributable to the glass network and the Gum Arabic polysaccharide component.

The carbonyl/carboxylate region showed the most pronounced changes among the five groups. The unmodified control (G1) exhibited a comparatively shallow absorption at 1582.8 cm^{-1} (minimum transmittance = 0.918). Following the addition of Gum Arabic alone (G2), this band shifted to 1629.7 cm^{-1} with increased absorption depth (minimum transmittance = 0.914). The most intense and sharply resolved absorption in this region across all groups was observed in G3 (1634.0 cm^{-1}, minimum transmittance = 0.746), representing the deepest overall absorption

recorded in the present study. G4 and G5 exhibited absorption depths intermediate between G2 and G3 (minimum transmittance = 0.865 and 0.894, respectively), with band positions at 1589.9 and 1581.4 cm^{-1}.

A progressive shift of the O–H stretching band toward lower wavenumbers was observed from the unmodified control (G1, 3396.0 cm^{-1}) through G2 (3367.5 cm^{-1}) to G3 (3343.4 cm^{-1}), the group containing the lowest garden cress oil concentration, consistent with progressively increased hydrogen bonding within the modified matrix at this concentration. Notably, this is also the group that subsequently demonstrated the highest compressive strength among all five formulations (Section 3.5), suggesting a coherent link between the spectroscopically observed matrix interaction and the bulk mechanical outcome.

To support interpretation of the composite cement spectra, FTIR reference spectra were additionally acquired for garden cress oil and Gum Arabic powder independently, prior to their incorporation into the GIC matrix. The reference spectrum of garden cress oil exhibited characteristic absorption bands consistent with a triglyceride-rich fixed oil, including a weak =C–H stretching band at 3009.2 cm^{-1} attributable to cis-unsaturated fatty acid chains, consistent with the documented alpha-linolenic acid content of Lepidium sativum oil, strong aliphatic CH_2 stretching at 2921.0 cm^{-1}, and a prominent, sharply resolved ester carbonyl (C=O) stretching band at 1746.4 cm^{-1}, the principal diagnostic marker of the triglyceride ester linkage. The reference spectrum of Gum Arabic powder exhibited a broad O–H stretching band at 3309.2 cm^{-1} attributable to the polysaccharide hydroxyl groups and an absorption band at 1601.3 cm^{-1} consistent with amide I and carboxylate asymmetric stretching of the arabinogalactan-protein complex. These reference assignments, together with the corresponding peak positions across G1–G5, are summarised in Table 3.

Direct comparison of the ester carbonyl diagnostic region (1700–1780 cm^{-1}) between the pure garden cress oil reference spectrum and the composite G1–G5 spectra revealed that the distinct, sharply resolved ester band observed at 1746.4 cm^{-1} in the pure oil was not similarly resolved as a discrete feature in any of the five composite cement groups, including G3, G4, and G5. Across all groups, transmittance in this region rose smoothly and monotonically from the dominant polyacrylate carbonyl/carboxylate absorption toward the spectral baseline, without a discernible local shoulder or secondary minimum near 1746 cm^{-1}. This finding likely reflects the relatively low fraction of garden cress oil within the set cement matrix combined with spectral overlap arising from the tail of the dominant, more intense native GIC carbonyl absorption in the same spectral region. Accordingly, evidence for garden cress oil incorporation

into the modified cement groups is derived primarily from the progressive changes in position and intensity of the O–H stretching and carbonyl/carboxylate bands described above, rather than from isolation of the oil's diagnostic ester band, and is considered together with, and corroborated by, the scanning electron microscopy and energy-dispersive X-ray findings presented in Sections 3.2 and 3.3.

3.2 Scanning Electron Microscopy (SEM) Analysis

The surface microstructure of the five experimental groups as examined by scanning electron microscopy at ×2000 magnification (**Figure 2**) revealed progressive and systematic changes in surface morphology with increasing garden cress oil concentration. The unmodified control (G1, **Figure 2A**) exhibited a moderately compact cement surface with scattered glass particles of variable size embedded within the polyacrylate matrix, alongside localized surface depressions consistent with the inherent porosity of the acid-base set glass ionomer cement. The surface of G2 (**Figure 2B**), modified with Gum Arabic alone, appeared notably smoother and more homogeneous than the control, with improved glass particle integration and fewer and shallower surface depressions, findings morphologically consistent with the significantly higher surface microhardness and reduced surface roughness recorded for this group. G3 (**Figure 2C**), incorporating Gum Arabic and garden cress oil at 0.5 vol.%, demonstrated a compact and relatively uniform surface without evidence of discrete oil droplet accumulation or phase separation at the surface, supporting the hypothesis that the Gum Arabic carrier system achieved homogeneous oil distribution within the cement matrix at this concentration. In contrast, G4 (**Figure 2D**) exhibited progressive surface deterioration characterized by the emergence of surface cracks, delamination zones, and structural discontinuities, providing a morphological basis for the significantly reduced compressive strength and surface microhardness observed in this group. G5 (**Figure 2E**), prepared with the highest oil concentration (1.5 vol.%), demonstrated the most severely disrupted surface morphology among all groups, with pronounced cracking, extensive delamination, and the appearance of rounded globular features consistent with surface-localized oil-rich regions, findings that are in full agreement with the lowest mechanical property values recorded across all tested parameters.

At higher magnification (×5000 and ×10000; **Figure 3.1 and 3.2** respectively), the microstructural differences among the five groups were further elucidated. The control group (G1, **Figure 3A**) demonstrated a smooth, compact polyacrylate matrix with sparsely distributed

glass particle remnants and no significant surface heterogeneity, serving as the morphological baseline for comparison. G2 (**Figure 3B**) revealed well-defined, rounded surface features with a compact and continuous matrix, reflecting the surface-enrichment effect of the hydrophilic Gum Arabic carrier during the aqueous setting phase, which appears to have contributed to the enhanced surface hardness and smoothness observed in this group. At ×5000 magnification, G3 (**Figure 3C**) showed a more complex surface texture with angular glass particles and inter-particle regions, yet crucially, no discrete spherical oil droplet features were identifiable at the surface, further corroborating the successful and homogeneous incorporation of garden cress oil into the cement matrix at 0.5 vol.% via the Gum Arabic emulsification system. In G4 (**Figure 3D**), the higher magnification revealed the co-existence of surface cracking and the early appearance of rounded globular features, suggesting that at 1.0 vol.% oil, the emulsification capacity of the fixed Gum Arabic concentration (0.5 wt.%) was beginning to be exceeded, resulting in a proportion of incompletely stabilized oil droplets accumulating at the cement surface and contributing to matrix disruption. The most striking finding at ×5000 magnification was observed in G5 (**Figure 3E**), which exhibited numerous, clearly defined, spherical features densely distributed across the surface, morphologically consistent with oil droplets that failed to be incorporated into the polyacrylate matrix due to the insufficient Gum Arabic emulsification capacity at 1.5 vol.% oil. The presence of these surface-localized oil-rich globules, combined with the extensive matrix disruption visible in this group, provides compelling morphological evidence for a concentration-dependent emulsification threshold beyond which the Gum Arabic carrier system at 0.5 wt.% is no longer capable of achieving stable, homogeneous oil distribution, directly explaining the progressive mechanical property deterioration observed from G3 through G5.

The scanning electron microscopic findings demonstrated a coherent and consistent correlation with the quantitative mechanical and surface property data across all five experimental groups. The compact, homogeneous surface morphology observed in G2 and G3 is in full agreement with the superior surface microhardness and reduced surface roughness recorded for these groups. The progressive surface deterioration, cracking, and oil droplet accumulation observed from G4 to G5 provide direct morphological explanation for the corresponding decline in compressive strength, surface microhardness, and increase in surface roughness. The absence of discrete oil droplet features in G3 and their progressive appearance and densification in G4 and G5 strongly support the existence of a concentration-dependent emulsification threshold at the fixed Gum Arabic carrier concentration employed (0.5 wt.%), beyond which

homogeneous oil incorporation into the cement matrix is no longer achievable. These findings collectively validate the central methodological premise of this study: that Gum Arabic at 0.5 wt.% constitutes an effective natural emulsification carrier for garden cress oil incorporation into conventional GIC specifically at 0.5 vol.% oil concentration, and that this optimal formulation (G3) achieves both the highest compressive strength and equivalent surface smoothness to the carrier-only group (G2), without the matrix disruption that characterizes higher oil concentrations.

3.3 Energy-Dispersive X-ray (EDX) Analysis

EDX elemental analysis was performed on the polished surface of representative specimens from all five experimental groups (three measurement points per group) to characterize the elemental composition of the cement surface and to identify diagnostic markers of oil and Gum Arabic incorporation. The elemental weight percentages (wt.%) recorded at each measurement point, together with group means and standard deviations, are summarised in Table 4. The phosphorus (P) detection pattern across individual measurement points is presented separately in Table 5 owing to its specific diagnostic significance.

The most diagnostically significant elemental findings concerned nitrogen (N) and phosphorus (P). Nitrogen was entirely absent from the unmodified control (G1, 0.00 ± 0.00 wt.%), confirming its complete absence from both conventional GIC and the unmodified polyacrylate matrix. A consistent nitrogen signal appeared in G2 (3.18 ± 0.43 wt.%), detected at all three measurement points, directly confirming the successful incorporation of Gum Arabic and specifically attributable to the arabinogalactan-protein complex of Gum Arabic, which is the sole nitrogen-bearing component introduced in this formulation. Nitrogen concentrations increased progressively through G3 (4.45 ± 0.31 wt.%), G4 (5.77 ± 1.34 wt.%), and G5 (13.45 ± 5.08 wt.%), a trend reflecting the progressive dilution and disruption of the inorganic glass-polyacrylate matrix at higher oil concentrations, which renders the organic Gum Arabic protein component proportionally more prominent at the specimen surface.

Phosphorus (P) was absent from both G1 and G2 (0.00 wt.% at all three measurement points in each group), consistent with the absence of any phosphate-containing component in either formulation. Phosphorus was detected in all three oil-containing groups (G3, G4, G5), attributable to the phospholipid and phosphate-containing minor lipid fraction of Lepidium sativum fixed oil. However, the pattern of phosphorus detection differed critically among the three oil groups and constitutes the most important EDX finding of the present study (Table 5).

In G3, phosphorus was detected consistently at all three measurement points (1.157, 1.167, and 0.824 wt.%), yielding the highest mean phosphorus content (1.05 ± 0.20 wt.%) and the lowest inter-point variability of all oil-containing groups. This consistent detection across the entire measured surface area is indicative of a homogeneous distribution of the oil phase within the cement matrix, providing direct elemental evidence for successful oil incorporation at the 0.5 vol.% concentration. In contrast, phosphorus was detected at only two of three measurement points in both G4 (0.922, 0.416, and 0.000 wt.%) and G5 (0.515, 0.000, and 0.274 wt.%), with substantially higher inter-point variability (SD = 0.462 and 0.258, respectively). The presence of measurement points recording zero phosphorus in G4 and G5 indicates that a proportion of the cement surface was devoid of detectable oil-derived phosphorus, while adjacent measurement points recorded phosphorus signals, a pattern consistent with non-uniform, clustered distribution of the oil phase at these concentrations.

The carbon (C) content increased progressively from G3 (16.30 ± 0.27 wt.%) through G4 (22.32 ± 3.76 wt.%) to G5 (36.87 ± 5.11 wt.%), directly reflecting the increasing contribution of garden cress oil fatty acid chains — which are predominantly composed of long-chain carbon structures — to the surface elemental composition at higher oil loadings. G2 recorded a slightly lower carbon signal than the control (12.93 vs 17.80 wt.%), attributable to point-to-point sampling variability with n = 3 measurement points rather than a genuine chemical reduction, as Gum Arabic itself is a carbon-containing polysaccharide. Fluorine (F), derived exclusively from the fluoroaluminosilicate glass phase, declined progressively from G3 onwards (9.42, 7.53, and 6.66 wt.% for G3, G4, and G5, respectively), reflecting the progressive dilution of the glass phase signal at the specimen surface as organic content increased. Similarly, aluminium (Al), silicon (Si), and calcium (Ca) — all components of the glass network and the polyacrylate cross-linked matrix — decreased markedly in G5, with Al falling from 13.09 wt.% in G1 to 5.31 wt.% in G5, and Ca from 11.87 wt.% to 6.67 wt.%, confirming progressive disruption and surface dilution of the inorganic cement matrix at the highest oil concentrations.

The EDX spectra for all five groups are presented in Figure 4. Collectively, the EDX findings are in complete agreement with, and provide chemical-level corroboration of, the mechanical, surface property, and scanning electron microscopic findings reported in the preceding sections. The elemental evidence specifically supports the interpretation that Gum Arabic at 0.5 wt.% achieves homogeneous oil distribution at 0.5 vol.% garden cress oil (G3), as evidenced by consistent phosphorus detection across all three surface measurement points, and

that this capacity is progressively exceeded at 1.0 and 1.5 vol.%, as evidenced by the heterogeneous, intermittent phosphorus detection pattern in G4 and G5.

3.4 Color Stability (ΔE)

The color stability of the five experimental groups was assessed by measuring the mean colour difference (ΔE) between each modified group (G2–G5) and the unmodified control (G1), which served as the reference (Table 6). A spectrophotometric assessment was performed on polished disc specimens under standardised illumination conditions. The unmodified control (G1) was designated as the reference baseline, and the ΔE values of the modified groups reflect the magnitude of colour deviation from this reference. The clinically relevant threshold for acceptability was set at $\Delta E < 3.3$, beyond which colour differences are considered clinically perceptible and unacceptable.

One-way ANOVA revealed a highly significant difference in colour deviation among the four modified groups (Table 7).

Post-hoc Tukey HSD comparisons (Table 8) demonstrated that all six pairwise comparisons among the modified groups were statistically significant ($p < 0.05$). G2 (Gum Arabic alone) exhibited the smallest mean colour deviation from the unmodified control ($\Delta E = 1.43 \pm 0.28$), representing a perceptible but clinically acceptable color difference. G3 ($\Delta E = 2.38 \pm 0.28$) and G4 ($\Delta E = 2.89 \pm 0.19$) likewise remained within the clinically acceptable range ($\Delta E < 3.3$), though their colour deviation from the control increased progressively with rising oil concentration. G5, prepared with the highest garden cress oil concentration (1.5 vol.%), demonstrated the greatest mean colour deviation ($\Delta E = 4.01 \pm 0.37$), significantly exceeding the clinically acceptable threshold of $\Delta E = 3.3$ and differing significantly from all other groups. A clear and monotonic dose-dependent increase in colour deviation was observed from G2 through G5, consistent with the progressive contribution of the naturally pigmented garden cress oil to the optical properties of the set cement matrix.

The color stability findings are in coherent agreement with the broader mechanical and surface property data. The progressive increase in ΔE with increasing oil concentration mirrors the parallel deterioration in compressive strength, surface microhardness, and surface roughness observed at higher oil fractions. Both the color and mechanical findings converge on the conclusion that G3 (0.5 vol.% garden cress oil) represents the optimal concentration, combining the highest compressive strength with a clinically acceptable color deviation, while

G5 consistently records the poorest performance across all outcome measures, including a clinically unacceptable colour change.

3.5 Compressive Strength

Mean compressive strength values, standard deviations, and Tukey HSD grouping are presented in Table 9, ranked from highest to lowest.

One-way ANOVA revealed a highly significant difference in compressive strength among the five groups (Table 10).

Post-hoc Tukey HSD comparisons (Table 11) showed that every pairwise group comparison reached statistical significance ($p < 0.05$), meaning all five groups were mutually and clearly distinguishable. G3 (0.5 vol.% garden cress oil) achieved the highest mean compressive strength (97.10 ± 3.75 MPa), significantly exceeding even the unmodified control (89.39 ± 3.13 MPa). G2 (Gum Arabic alone, 80.98 ± 4.49 MPa) was significantly lower than both the control and G3, indicating that Gum Arabic alone does not enhance — and may modestly reduce — bulk compressive strength in the absence of the oil phase. Compressive strength declined sharply and progressively at higher garden cress oil concentrations, with G4 (39.22 ± 2.61 MPa) and G5 (22.74 ± 1.82 MPa) falling far below every other group.

3.6 Surface Microhardness

Mean surface microhardness values, standard deviations, and Tukey HSD grouping are presented in Table 12, ranked from highest to lowest.

One-way ANOVA revealed a highly significant difference in surface microhardness among the five groups (Table 13).

Post-hoc Tukey HSD comparisons (Table 14) demonstrated that all pairwise group comparisons were statistically significant ($p < 0.05$). G2 (Gum Arabic alone) exhibited the highest surface microhardness (73.33 ± 2.56 VHN), significantly exceeding every other group, including G3 (56.29 ± 3.83 VHN), which ranked second. Both G2 and G3 significantly exceeded the unmodified control (44.40 ± 3.99 VHN). Microhardness declined below control values at the two higher garden cress oil concentrations, with G4 (37.84 ± 2.01 VHN) and G5 (29.75 ± 2.00 VHN) recording the lowest values among all groups. This pattern — G2 outperforming G3 at the surface despite G3 outperforming G2 in bulk compressive strength (Section 3.5) — is addressed in the Discussion in terms of differential surface-versus-bulk partitioning of the hydrophilic Gum Arabic carrier.

3.7 Surface Roughness

Mean surface roughness (Ra) values, standard deviations, and Tukey HSD grouping are presented in Table 15, ranked from lowest (smoothest) to highest (roughest).

One-way ANOVA revealed a highly significant difference in surface roughness among the five groups (Table 16).

Post-hoc Tukey HSD comparisons (Table 17) showed that G2 (0.488 ± 0.053 μm) and G3 (0.496 ± 0.062 μm) did not differ significantly from one another ($p = 0.9997$) and both demonstrated significantly smoother surfaces than every other group. Similarly, the unmodified control (G1, 0.814 ± 0.065 μm) and G4 (0.699 ± 0.084 μm) did not differ significantly from one another ($p = 0.078$). G5 exhibited the highest and most variable surface roughness (1.058 ± 0.171 μm), significantly exceeding all other groups. The convergence of G2 and G3 at the smoothest end of the spectrum mirrors their convergence at the upper end of the microhardness ranking, supporting a consistent surface-level explanation for both properties. Compressive strength, surface microhardness and surface roughness are graphically presented in Figure 5.

4. Discussion

4.1 Overview of Principal Findings

The present study examined the effect of incorporating Lepidium sativum fixed oil into conventional glass ionomer cement at three concentrations (0.5, 1.0, and 1.5 vol.%) using Gum Arabic as a natural carrier. The four outcomes investigated — compressive strength, surface microhardness, surface roughness, and color stability — all revealed statistically significant concentration-dependent effects, with the lowest oil concentration (G3, 0.5 vol.%) consistently yielding the most favorable or comparable property profile relative to the unmodified control. This pattern — improvement or maintenance of properties at the lowest modification concentration followed by progressive deterioration at higher concentrations — has been described in comparable studies examining the incorporation of bioactive agents into glass ionomer cement formulations, and represents a recurring theme in the natural agent modification literature that underlines the importance of systematic dose–response evaluation.

4.2 FTIR Spectroscopic Findings

FTIR spectroscopy provided chemical-level evidence for the interactions occurring within the modified cement matrix. The most informative change was observed in the carbonyl/carboxylate absorption region (1580–1640 cm^{-1}), in which G3 exhibited the deepest and most sharply resolved absorption of all five cement groups (minimum transmittance = 0.746; band position 1634.0 cm^{-1}). This observation is consistent with the most extensive coordination between polyacrylate carboxylate groups and calcium ions leached from the glass phase during the acid–base setting reaction at this concentration — a process central to the cross-linked network structure that determines mechanical integrity in set GIC. A progressive red-shift of the O–H stretching band from G1 (3396.0 cm^{-1}) through G2 (3367.5 cm^{-1}) to G3 (3343.4 cm^{-1}) further indicates increasing hydrogen bonding interactions within the modified cement network at the lowest oil concentration, consistent with greater structural cohesion.

Reference spectra independently acquired for garden cress oil and Gum Arabic powder confirmed the band assignments employed in the composite spectral analysis. The diagnostic triglyceride ester carbonyl band of the oil (1746.4 cm^{-1}) was not resolved as a discrete feature in the composite G1–G5 spectra, a result attributable to the low oil fraction relative to the dominant polyacrylate absorption in this spectral region. This spectroscopic limitation is acknowledged, and evidence for oil incorporation in the present study is derived from the systematic pattern of chemical changes across the five groups alongside the SEM morphological findings described below.

4.3 Scanning Electron Microscopic Findings

SEM at ×2000, ×5000 and ×10000 magnifications revealed progressive and systematic surface morphological changes consistent with the quantitative mechanical data. The unmodified control (G1) demonstrated baseline GIC surface morphology with a moderately compact polyacrylate matrix, scattered glass particles, and localised surface depressions. G2 (Gum Arabic alone) displayed a notably smoother and more continuous surface, providing morphological support for its significantly superior surface microhardness and reduced roughness. G3 exhibited a compact, uniform surface without identifiable discrete oil-phase features at either magnification, indicating homogeneous distribution of the oil within the cement matrix at 0.5 vol.%. In contrast, G4 and G5 demonstrated progressively more severe surface disruption, including cracking, delamination, and — at ×5000 and ×10000 magnifications — rounded globular features morphologically consistent with phase-separated oil regions accumulating at the cement surface. The density of these features increased from

G4 to G5, directly paralleling the stepwise mechanical property deterioration recorded quantitatively for these groups.

4.4 Compressive Strength

Compressive strength is the primary mechanical benchmark for restorative dental cements under ISO 9917-1:2007, which specifies a minimum of 100 MPa for Type II restorative GIC [ISO 9917-1]. The unmodified control (89.39 MPa), consistent with published values for conventional GIC formulations under comparable laboratory testing conditions. G3 (97.10 MPa) significantly exceeded the control, is a notable finding for a natural agent modification

prepared without chemical synthesis. G2 (Gum Arabic alone, 80.98 MPa) produced compressive strength significantly below both the control and G3, establishing that the mechanical improvement in G3 is attributable to the combined effect of the oil and Gum Arabic, not to the carrier alone.

The mechanism by which low-concentration fixed oil incorporation may enhance compressive strength is not fully resolved. The FTIR data showing the strongest carbonyl absorption in G3 — consistent with maximum matrix chemical interaction at this concentration — support the interpretation that the oil modifies the setting dynamics of the polyacrylate phase, facilitating more complete ionic cross-linking between the polyacid and calcium ions from the glass at this specific concentration. Analogous compressive strength enhancements at low natural agent concentrations have been reported in the GIC modification literature, where fixed and essential oils have similarly demonstrated beneficial mechanical effects at low loading fractions. The dramatic decline in compressive strength at G4 (39.22 MPa) and G5 (22.74 MPa) is directly explained by the SEM-evidenced phase separation of oil at higher concentrations, which disrupts the continuity of the polyacrylate network and introduces macroscopic structural discontinuities acting as stress concentration points [15,16, 22,23,34].

4.5 Surface Microhardness

Surface microhardness reflects the resistance of the outermost cement layer to indentation and is relevant to the clinical wear resistance of the restoration surface [2]. The highest microhardness was recorded for G2 (73.33 VHN), significantly exceeding both the control (44.40 VHN) and G3 (56.29 VHN). This divergence from the compressive strength hierarchy — where G3 ranked highest and G2 ranked below the control — is one of the most

mechanistically interesting findings of the present study and reflects a differential effect of the modification on surface-confined versus bulk properties.

A reasonable explanation lies in the hydrophilic nature of Gum Arabic. During the aqueous setting phase of conventional GIC, the arabinogalactan-protein complex of Gum Arabic — being highly water-compatible relative to both the inorganic glass and the polyacrylate chain — may preferentially concentrate toward the specimen surface as the aqueous medium is progressively consumed by the acid–base reaction. This surface enrichment would logically enhance surface microhardness and smoothness (both of which are superior in G2) without proportionally improving bulk compressive strength [3,31,35,36]. In G3, the simultaneous presence of a hydrophobic oil phase may partially disrupt this surface partitioning, redistributing the Gum Arabic effect more uniformly through the bulk matrix — which would account for G3's bulk compressive strength superiority. The decline in microhardness in G4 and G5 to below control values is consistent with structural disruption of the surface layer by phase-separated oil, as evidenced by the SEM findings [22,23].

4.6 Surface Roughness

Surface roughness is a clinically relevant parameter because elevated Ra values promote bacterial adhesion and plaque accumulation. A Ra threshold of approximately 0.2 μm, below which surface roughness has minimal additional influence on bacterial adhesion, has been identified in the periodontal literature [37]. All groups in the present study exceeded this threshold, consistent with published Ra values for conventionally polished conventional GIC specimens in *in vitro* settings [1, 2] and reflecting the intrinsic surface texture of the polished cement matrix. Nevertheless, G2 (0.488 μm) and G3 (0.496 μm) produced significantly smoother surfaces than the unmodified control (0.814 μm), a clinically meaningful relative improvement. The statistical non-significance of the difference between G2 and G3 ($p = 0.9997$) mirrors their similar performance at the microhardness level, reinforcing the surface-enrichment mechanism proposed above. G5 (1.058 μm) recorded the highest and most variable roughness, consistent with the gross surface disruption visible in the SEM micrographs [23,31,36].

4.7 Color Stability

Color deviation (ΔE) was measured as the chromatic difference between each modified group and the unmodified control. The clinically accepted acceptability threshold for dental restorative materials is $\Delta E < 3.3$, representing the upper limit within which colour differences

between a restoration and a reference are considered clinically tolerable [38]. G2 (1.43 ± 0.28) and G3 (2.38 ± 0.28) produced colour deviations well within this threshold, as did G4 (2.89 ± 0.19), while G5 (4.01 ± 0.37) significantly exceeded it. The monotonically increasing ΔE from G2 through G5 constitutes the most clearly dose-dependent pattern recorded in the present study and is attributable to the progressive contribution of the naturally pale-yellow pigmentation of garden cress oil — a consequence of its fatty acid and phytochemical composition [39,40] — to the optical appearance of the set cement.

The fact that G5's colour deviation exceeds the clinical acceptability threshold reinforces its unsuitability for restorative application, consistent with all other outcome measures recorded for this group. For G3, the combination of clinically acceptable colour deviation (ΔE = 2.38), the highest compressive strength, and a smooth surface positions it as the formulation with the most favorable overall property profile in the present study.

4.8 Energy-Dispersive X-ray (EDX) Analysis

EDX elemental analysis provided chemical-level corroboration of the mechanical, surface property, and scanning electron microscopic findings reported in the preceding sections. The most diagnostically significant findings concerned two elements absent from the unmodified control: nitrogen (N), derived from the arabinogalactan-protein complex of Gum Arabic, and phosphorus (P), attributable to the phospholipid and phosphate-containing minor lipid fraction of Lepidium sativum fixed oil.

Nitrogen was completely absent from G1 (0.00 ± 0.00 wt.%), confirming the absence of any protein-bearing component in the unmodified cement. Its consistent detection in G2 (3.18 ± 0.43 wt.%) and in all subsequent oil-containing groups confirms Gum Arabic incorporation across all modified formulations. The progressive increase in nitrogen from G2 through G5 (13.45 ± 5.08 wt.%) is interpreted as a relative enrichment of the Gum Arabic protein fraction at the cement surface, consequent upon the progressive disruption and dilution of the inorganic glass-polyacrylate matrix at higher oil concentrations, rather than an absolute increase in Gum Arabic content, which was fixed at 0.5 wt.% across all modified groups.

The phosphorus detection pattern constitutes the most important EDX finding in relation to the central research question of this study. Phosphorus was absent from both G1 and G2, as expected in the absence of any phosphate-containing component. In G3, phosphorus was detected at all three measurement points (1.157, 1.167, and 0.824 wt.%), yielding the highest mean phosphorus content of all oil-containing groups (1.05 ± 0.20 wt.%) and the lowest inter-

point variability. This consistent, low-variability detection across the entirety of the measured surface area constitutes direct elemental evidence that the oil phase was distributed homogeneously within the cement matrix at 0.5 vol.%, supporting the interpretation of successful Gum Arabic-mediated oil incorporation at this concentration. The EDX finding thus provides chemical-level confirmation of what the SEM morphological data demonstrated visually: the absence of discrete oil-phase features on the G3 surface is explained by genuinely homogeneous microscale oil distribution, not by the absence of oil. In G4 and G5, phosphorus was detected at only two of three measurement points, with substantially higher inter-point variability (SD = 0.462 and 0.258, respectively, versus 0.195 for G3). The measurement points recording zero phosphorus in these groups indicate that portions of the cement surface contained no detectable oil-derived phosphorus, while immediately adjacent areas did, a pattern that is the elemental fingerprint of phase-separated, clustered oil distribution. This elemental heterogeneity directly corroborates the rounded globular surface features observed in SEM for G4 and G5, and provides a chemical explanation for the declining mechanical properties at these concentrations: clustered, non-homogeneous oil distribution creates both structural discontinuities in the cement matrix and an uneven surface composition, neither of which is conducive to mechanical integrity or surface cohesion.

The carbon (C) trend, increasing progressively from G3 (16.30 wt.%) through G4 (22.32 wt.%) to G5 (36.87 wt.%), reflects the growing contribution of garden cress oil fatty acid chains to the surface elemental composition at higher loadings and provides independent quantitative confirmation of the increasing oil presence in these groups. The parallel decline in fluorine (F), aluminium (Al), silicon (Si), and calcium (Ca) from G4 onwards confirms the progressive surface dilution of the glass-polyacrylate network by organic material, consistent with the SEM evidence of matrix disruption and the mechanical data showing declining compressive strength and microhardness. Taken together, the EDX findings are fully consistent with all other outcomes of this study and strengthen the mechanistic conclusion that 0.5 wt.% Gum Arabic achieves homogeneous oil distribution at 0.5 vol.% garden cress oil but is insufficient to prevent phase separation at the higher oil concentrations employed.

4.9 Comparison with Prior GIC Modification Literature

The present findings are in broad agreement with the emerging body of literature investigating the incorporation of plant-derived bioactive agents into conventional GIC, in which low-

concentration modification has been associated with mechanical improvement while higher concentrations produce matrix disruption and property deterioration [1, 2].

The specific choice of Lepidium sativum as the bioactive oil in the present study is justified by its documented phytochemical composition, characterised by high content of alpha-linolenic acid (an omega-3 unsaturated fatty acid), alongside oleic acid and other bioactive constituents [26-28]. These components have been associated with antioxidant and antimicrobial activities in the pharmacological literature [25], properties that, if retained following incorporation into the cement matrix, could confer biological benefits beyond the mechanical improvements documented here. However, formal evaluation of these potential biological effects — including antibacterial activity against caries-associated organisms and cytotoxicity assessment — falls outside the scope of the present study and is recommended for subsequent investigation.

4.10 Role of Gum Arabic

The independent contribution of Gum Arabic to the GIC property profile, assessed via the G2 group (Gum Arabic alone), is itself a substantive finding. G2 demonstrated the highest surface microhardness and smoothest surface of all five groups while recording compressive strength below the control, a differential behaviour that underscores the importance of including a carrier-only control group in modification studies of this type. Without G2, it would not be possible to separate the contributions of the oil and the carrier to the observed effects in G3. Gum Arabic is a complex arabinogalactan-protein complex with well-documented surface-active and film-forming properties [31,35,36], and its preferential surface partitioning during the aqueous GIC setting phase — as proposed above to explain G2's surface superiority — is consistent with the physicochemical behaviour of hydrophilic macromolecules in aqueous cement systems. The inclusion of G2 as an independent carrier control is considered a methodological strength of the present study design.

5. Conclusion

Within the limitations of this *in vitro* study, the following conclusions may be drawn. The incorporation of Lepidium sativum fixed oil at 0.5 vol.% into conventional glass ionomer cement using Gum Arabic as a natural carrier (G3) significantly enhanced compressive strength

relative to the unmodified control, while simultaneously maintaining clinically acceptable surface microhardness, surface smoothness, and color stability. Gum Arabic alone (G2) produced the highest surface microhardness and the smoothest surface of all groups but did not improve bulk compressive strength, reflecting a differential surface-versus-bulk modification effect attributed to the hydrophilic partitioning behaviour of the carrier during cement setting. Color stability followed a strictly dose-dependent pattern; groups G2, G3, and G4 remained within the clinically acceptable colour deviation threshold ($\Delta E < 3.3$), while G5 (1.5 vol.%) exceeded it, further disqualifying higher oil concentrations from clinical consideration. FTIR spectroscopic and SEM morphological findings provided coherent chemical and microstructural corroboration for the observed mechanical outcomes across all five groups. The present results collectively identify G3 as the optimal formulation in this in vitro investigation. Clinical translation of this formulation requires the completion of biological evaluation, including cytotoxicity testing, antibacterial efficacy assessment, and fluoride release quantification, together with simulation of long-term oral ageing conditions.

6. Clinical Implications

The findings of the present study carry several implications for the clinical application of bioactive-modified glass ionomer cements. The significant compressive strength enhancement achieved in G3 without adverse effect on surface properties or color acceptability addresses one of the principal mechanical limitations of conventional GIC in restorative dentistry. If reproducible under biological and long-term ageing conditions, this modification could extend the utility of conventional GIC to clinical situations requiring greater mechanical resistance, including small posterior restorations and high-caries-risk patients in whom the fluoride release benefit of GIC is particularly valuable.

The color acceptability of G3 ($\Delta E = 2.38$, within the $\Delta E < 3.3$ clinical threshold) is directly relevant to aesthetic restorative applications. The modification does not produce a macroscopically visible or clinically unacceptable chromatic change, meaning that the aesthetic performance of the cement is not compromised by oil incorporation at the optimal concentration. This finding is important for anterior restorations and for patients with elevated esthetic expectations, where color fidelity is a primary clinical requirement.

The use of Gum Arabic as the carrier component in this formulation is clinically relevant because of its established safety profile in food and pharmaceutical applications. Its documented biocompatibility — consistent with its classification as an accepted excipient in

multiple pharmacopoeias— supports its candidacy for dental applications, pending formal in vitro cytotoxicity confirmation in the oral biomaterial context.

The concentration-dependent deterioration observed at 1.0 and 1.5 vol.% carries a direct practical message: the benefit of natural agent incorporation is highly concentration-sensitive, and exceeding the effective window rapidly reverses any mechanical or surface advantage while also producing unacceptable color deviation. This finding reinforces the necessity of systematic in vitro dose–response evaluation prior to any clinical translation of bioactive GIC modifications.

7. Limitations

The following study limitations should be considered when interpreting the present findings. First, all testing was conducted under standardized *in vitro* laboratory conditions, which do not fully replicate the thermal cycling, masticatory mechanical loading, salivary enzymatic activity, and microbial environment of the oral cavity. Long-term performance of the modified formulations under simulated clinical conditions requires separate evaluation.

Second, EDX elemental analysis was performed at three measurement points per specimen per group. While this provided sufficient resolution to identify the key diagnostic elemental differences among groups — particularly the uniform versus heterogeneous phosphorus distribution pattern — a larger number of measurement points or full surface elemental mapping would provide a more comprehensive spatial profile and is recommended for future work.

Third, the biological performance profile of the modified formulations — including antibacterial activity against cariogenic and periodontal organisms, in vitro cytotoxicity, and fluoride release kinetics — was not assessed in the present study. These represent necessary prerequisites for clinical translation and are priorities for subsequent investigation.

Fourth, the study employed a single commercially available conventional GIC. Extrapolation of findings to other conventional GIC formulations with different powder particle size distributions, powder/liquid ratios, or polyacid molecular weights should not be assumed without direct experimental verification.

References

1. Wilson AD, Kent BE. A new translucent cement for dentistry. The glass ionomer cement. Br Dent J. 1972;132(4):133-135. doi:10.1038/sj.bdj.4802810.
2. Mount GJ. Glass-ionomer cements: past, present and future. Oper Dent. 1994;19(3):82-90.

3. Nicholson JW. Chemistry of glass-ionomer cements: a review. Biomaterials. 1998;19(6):485-494. doi:10.1016/S0142-9612(97)00128-2.
4. Cho SY, Cheng AC. A review of glass ionomer restorations in the primary dentition. J Can Dent Assoc. 1999;65:491-495.
5. Frankenberger R, Sindel J, Kramer N. Viscous glass-ionomer cements: a new alternative to amalgam in the primary dentition? Quintessence Int. 1997;28:667-676.
6. Berg JH. The continuum of restorative materials in pediatric dentistry: a review for the clinician. Pediatr Dent. 1998;20:93-100.
7. Peutzfeldt A, García-Godoy F, Asmussen E. Surface hardness and wear of glass ionomers and compomers. Am J Dent. 1997;10(1):15-17.
8. Nicholson JW, Sidhu SK, Czarnecka B. The effect of drying on the surface hardness of glass-ionomer dental cements. J Appl Biomater Funct Mater. 2015;13(2):e105-e108.
9. Ferracane JL. Resin composite—state of the art. Dent Mater. 2011;27(1):29-38.
10. Khoroushi M, Keshani F. A review of glass-ionomers: from conventional glass-ionomer to bioactive glass-ionomer. Dent Res J (Isfahan). 2013;10(4):411-420.
11. Francisconi LF, Scaffa PM, de Barros VR, Coutinho M, Francisconi PA. Glass ionomer cements and their role in the restoration of non-carious cervical lesions. J Appl Oral Sci. 2009;17(5):364-369.
12. Lohbauer U. Dental glass ionomer cements as permanent filling materials?—Properties, limitations and future trends. Materials (Basel). 2010;3(1):76-96. doi:10.3390/ma3010076.
13. Moshaverinia A, Roohpour N, Chee WWL, Schricker SR. A review of powder modifications in conventional glass-ionomer dental cements. J Mater Chem. 2011;21:1319-1328. doi:10.1039/C0JM02309D.
14. Moshaverinia A, Roohpour N, Chee WWL, Schricker SR. A review of polyelectrolyte modifications in conventional glass-ionomer dental cements. J Mater Chem. 2012;22:2824-2833. doi:10.1039/C2JM14880C.
15. Aref NS. Sesame oil (Sesamum indicum L.) as a new challenge for reinforcement of conventional glass ionomer cement, could it be? Int J Dent. 2021;2021:5516517. doi:10.1155/2021/5516517.
16. Aref NS, Abdallah RM. Could different formulations of grape seed (Vitis vinifera) influence the physical properties of conventional glass ionomer cement? Contemp Clin Dent. 2021;12(4):383-388. doi:10.4103/ccd.ccd_696_20.
17. Aref NS, El-Fallal AA, El-Farrash MA, Reicha FM, Al-Wakeel EE. Compositional design and formulation study of hydroxyapatite-chitosan nanocomposite-modified conventional

glass ionomer cement: influence of composition and loading on mechanical, interfacial, and antibacterial properties. BMC Oral Health. 2026;26(1):1062. doi:10.1186/s12903-026-08797-3.

18. Azimi R, Shahgholi M, Khandan A. Fabrication and characterization of reinforced glass ionomer cement by zinc oxide and hydroxyapatite nanoparticles. Heliyon. 2024;10(20):e39063. doi:10.1016/j.heliyon.2024.e39063.
19. Garcia-Contreras R, Scougall-Vilchis RJ, Contreras-Bulnes R, Sakagami H, Morales-Luckie RA, Nakajima H. Mechanical, antibacterial and bond strength properties of nano-titanium-enriched glass ionomer cement. J Appl Oral Sci. 2015;23(3):321-328.
20. Moshaverinia A, Roohpour N, Darr JA, Rehman IU. Synthesis and characterization of a novel N-vinylcaprolactam-containing acrylic acid terpolymer for applications in glass-ionomer dental cements. Acta Biomater. 2009;5(6):2101-2108. doi:10.1016/j.actbio.2009.02.015.
21. Ezzat D, Azab A, Kamel IS, et al. Phytomedicine and green nanotechnology: enhancing glass ionomer cements for sustainable dental restorations: a comprehensive review. Beni Suef Univ J Basic Appl Sci. 2025;14:48. doi:10.1186/s43088-025-00633-x.
22. Paulraj J, Pushparathna B, Maiti S, Sharma N, Shanmugam R. A comparative in vitro analysis of antimicrobial effectiveness and compressive strength of ginger- and clove-modified glass ionomer cement. Cureus. 2024;16(3):e55964. doi:10.7759/cureus.55964.
23. Sherief DI, Fathi MS, Abou El Fadl RK. Antimicrobial properties, compressive strength and fluoride release capacity of essential oil-modified glass ionomer cements: an in vitro study. Clin Oral Investig. 2021;25(4):1879-1888. doi:10.1007/s00784-020-03493-0.
24. Tanudjaja HJ, Hejase CA, Tarabara VV, Fane AG, Chew JW. Membrane-based separation for oily wastewater: a practical perspective. Water Res. 2019;156:347-365.
25. Hekmatshoar Y, Özkan T, Rahbar Saadat Y. Evidence for health-promoting properties of Lepidium sativum L.: an updated comprehensive review. Turk J Pharm Sci. 2022;19(6):714-723. doi:10.4274/tjps.galenos.2021.07504.
26. Baregama C, Goyal A. Phytoconstituents, pharmacological activity, and medicinal use of Lepidium sativum Linn.: a review. Asian J Pharm Clin Res. 2019;12:45-50.
27. Jain T, Grover K. A comprehensive review on the nutritional and nutraceutical aspects of garden cress (Lepidium sativum Linn.). Proc Natl Acad Sci India Sect B Biol Sci. 2018;88:829-836.
28. Sat IG, Yildirim E, Turan M, Demirbas M. Antioxidant and nutritional characteristics of garden cress (Lepidium sativum). Acta Sci Pol Hortorum Cultus. 2013;12:173-179.

29. Zia-Ul-Haq M, Ahmad S, Calani L, Mazzeo T, Del Rio D, Pellegrini N, et al. Compositional study and antioxidant potential of Ipomoea hederacea Jacq. and Lepidium sativum L. seeds. Molecules. 2012;17(9):10306-10321. doi:10.3390/molecules170910306.
30. Thévenet F. Acacia gum (gum arabic). In: Phillips GO, Williams PA, editors. Handbook of Hydrocolloids. 2nd ed. Cambridge: Woodhead Publishing; 2009. **ISBN:** 978-1-84569-414-2.
31. Williams PA, Phillips GO. Gum arabic. In: Phillips GO, Williams PA, editors. Handbook of Hydrocolloids. 2nd ed. Cambridge: Woodhead Publishing; 2009. p. 252-273.
32. Jalali-Jivan M, Nejatian M, Capanoglu E, Fathi M, Tomas M, Gunal-Koroglu D, et al. Gum Arabic as a functional biopolymer: from fundamental properties to emerging encapsulation of nutraceuticals and bioactive compounds. Carbohydr Polym Technol Appl. 2026;14,101129. doi.org/10.1016/j.carpta.2026.101129.
33. Mohamed SA, Elsherbini AM, Alrefaey HR, Adelrahman K, Moustafa A, Egodawaththa NM, et al. Gum Arabic: a commodity with versatile formulations and applications. Nanomaterials (Basel). 2025;15(4):290. doi:10.3390/nano15040290.
34. Leal-Calderon F, Schmitt V, Bibette J. Emulsion Science: Basic Principles. 2nd ed. New York: Springer; 2007.
35. Castellani O, Guibert D, Al-Assaf S, Axelos MAV, Phillips GO, Anton M. Hydrocolloids with emulsifying capacity. Part 1: Emulsifying properties and interfacial characteristics of conventional (Acacia senegal (L.) Willd. var. senegal) and matured (Acacia sen SUPER GUM™) Acacia senegal. Food Hydrocoll. 2010;24(2-3):193-199. doi:10.1016/j.foodhyd.2009.09.005.
36. Gomes FP, Rocha SC, Coelho MAZ, Pereira AG, Coimbra MA. Lipid/particle assemblies based on maltodextrin-gum arabic core as bio-carriers. Colloids Surf B Biointerfaces. 2010;76(1):292-299. doi:10.1016/j.colsurfb.2009.12.004.
37. Quirynen M, Bollen CML. The influence of surface roughness and surface-free energy on supra- and subgingival plaque formation in man: a review of the literature. J Clin Periodontol. 1995;22(1):1-14.
38. Paravina RD, Ghinea R, Herrera LJ, Alvarez-Evallar AD, Lone M, Vargas M, et al. Color difference thresholds in dentistry. J Esthet Restor Dent. 2015;27(Suppl 1):S1-S9.
39. Gokavi SS, Malleshi NG, Guo M. Chemical composition of garden cress (Lepidium sativum) seeds and its fractions and use of bran as a functional ingredient. Plant Foods Hum Nutr. 2004;59(3):105-111.

40. Prajapati R, Kalariya M, Umbarkar R, Parmar S, Sheth N. Lepidium sativum: an overview of its nutritional and pharmacological profile. Asian J Pharm Sci. 2010;5(5):207-214.

Table 1. Experimental group composition.

Group	Designation	Composition	Scientific Purpose
G1	**Control GIC**	Conventional GIC — Fuji IX GP, (powder/liquid)	Unmodified baseline reference
G2	**GIC + Gum Arabic**	GIC liquid + 0.5 wt.% Gum Arabic, no oil	Isolates the independent effect of the Gum Arabic carrier
G3	**GIC + GA + GCO 0.5 vol.%**	GIC liquid + Gum Arabic + 0.5 vol.% garden cress oil	Low-concentration evaluation
G4	**GIC + GA + GCO 1.0 vol.%**	GIC liquid + Gum Arabic + 1.0 vol.% garden cress oil	Mid-concentration evaluation
G5	**GIC + GA + GCO 1.5 vol.%**	GIC liquid + Gum Arabic + 1.5 vol.% garden cress oil	High-concentration evaluation

Table 2. Outcome measures, specimen details, and applicable standards.

Domain	Outcome Measure	Specimen Dimensions	n per Group	Standard
Characterization	FTIR spectroscopy	Powdered set specimens	3	ATR-FTIR
Characterization	SEM — surface morphology	Intact, non-fractured discs	3 representative	—
Characterization	EDX — elemental mapping	Same discs as SEM	3 representative	—
Mechanical	Compressive strength (MPa)	Cylinders: 6 mm ⌀ × 4 mm H	10	ISO 9917-1
Surface Mechanical	Surface microhardness (VHN)	Discs: 10 mm ⌀ × 2 mm H	10	ISO 6507-1
Surface	Surface roughness, Ra (µm)	Same discs as microhardness	10	ISO 4287
Optical	Color stability (ΔE)	Same discs as microhardness	10	CIE L*a*b*

Table 3. Verified FTIR peak positions (cm^{-1}) extracted from raw spectral data — reference components and experimental groups.

Spectral Region	GCO	GA	G1	G2	G3	G4	G5	Tentative Assignment
O–H stretch	—	3309.2	3396.0	3367.5	3343.4	3387.4	3363.3	Hydroxyl/adsorbed water (broad in GA); progressive red-shift G1→G3 indicates increased hydrogen bonding
=C–H stretch (unsaturation)	**3009.2**	—	—	—	—	—	—	cis-Unsaturated fatty acid marker — unique to garden cress oil (e.g. alpha-linolenic acid)
Aliphatic C–H stretch	**2921.0**	2918.2	2922.4	2922.4	2922.4	2925.3	2923.8	CH_2 asymmetric stretch — strongest in pure oil, present at lower intensity in all cement groups
Ester C=O stretch	**1746.4**	—	—	—	—	—	—	Triglyceride ester carbonyl — diagnostic marker unique to garden cress oil; not resolved as a discrete feature in composite spectra (see Note)

Carbonyl/carboxylate region	—	1601.3	1582.8	1629.7	1634.0	**1589.9**	1581.4	Amide I/carboxylate (GA); polyacrylate C=O/COO^- (GIC groups); strongest, sharpest absorption in G3
C–H bending	**1459.1**	—	1456.2	1456.2	1456.2	—	1454.8	CH_2/CH_3 bending
COO^- symmetric stretch	—	—	1405.0	1405.0	1402.2	1403.6	1405.0	Polyacrylate carboxylate symmetric stretch — consistent across all GIC groups
Si–O–Si / C–O	1025.3	1018.2	1036.7	1023.9	1026.8	1038.1	1033.9	Glass network Si–O–Si and Gum Arabic C–O–C polysaccharide stretch (overlapping in modified groups)
Minimum transmittance	0.546	0.653	0.918	0.914	**0.746**	0.865	0.894	Overall absorption intensity — G3 shows the strongest absorption among the five cement groups

Table 4. EDX elemental composition (mean ± SD, wt.%) of the five experimental groups (n = 3 measurement points per group).

El.	Element	G1	G2	G3	G4	G5	Assignment / Trend
C	Carbon	17.80 ± 0.46	12.93 ± 0.51	16.30 ± 0.27	22.32 ± 3.76	36.87 ± 5.11	Polyacrylate matrix + oil fatty acid chains; increases markedly G3→G5
N	Nitrogen	0.00 ± 0.00	3.18 ± 0.43	4.45 ± 0.31	5.77 ± 1.34	13.45 ± 5.08	Gum Arabic protein fraction; absent in control, present G2–G5
O	Oxygen	38.36 ± 0.50	36.99 ± 0.52	34.49 ± 0.29	33.02 ± 1.34	25.85 ± 2.60	All components; decreases as organic content rises
F	Fluorine	11.31 ± 0.85	11.69 ± 0.52	9.42 ± 0.27	7.53 ± 1.14	6.66 ± 1.19	Fluoroaluminosilicate glass; decreases with progressive glass phase dilution
Al	Aluminium	13.09 ± 0.61	12.73 ± 0.21	12.70 ± 0.37	11.03 ± 1.40	5.31 ± 2.02	Glass network; stable G1–G3, declines G4–G5
Si	Silicon	7.58 ± 1.29	9.23 ± 0.43	8.07 ± 0.73	8.53 ± 1.15	4.93 ± 2.26	Glass network; relatively stable G1–G4, declines sharply G5
Ca	Calcium	11.87 ± 0.29	13.25 ± 0.59	13.53 ± 0.84	11.36 ± 2.13	6.67 ± 3.29	Glass phase + polyacrylate cross-links; markedly reduced G5
P	Phosphorus	0.00 ± 0.00	0.00 ± 0.00	**1.05 ± 0.20**	0.45 ± 0.46	0.26 ± 0.26	Garden cress oil marker; absent G1–G2; uniform G3 (3/3 pts); uneven G4–G5 (2/3 pts)

Note. Values are mean ± SD of weight percent (wt.%) at three measurement points per group. El. = element symbol. G1 = unmodified control; G2 = GIC + Gum Arabic; G3–G5 = GIC + Gum Arabic + 0.5, 1.0, and 1.5 vol.% garden cress oil, respectively. Bold values in G3 (P row) indicate the highest and most consistent phosphorus signal. Bold values in N row indicate elements diagnostic of Gum Arabic incorporation.

Table 5. Phosphorus (P) detection pattern across three measurement points per group (wt.%).

Group	Point 1 (wt.%)	Point 2 (wt.%)	Point 3 (wt.%)	Mean ± SD	Detection
G1	0.000	0.000	0.000	0.00 ± 0.00	0 / 3 points
G2	0.000	0.000	0.000	0.00 ± 0.00	0 / 3 points

Group	Point 1 (wt.%)	Point 2 (wt.%)	Point 3 (wt.%)	Mean ± SD	Detection
G3	**1.157**	**1.167**	**0.824**	**1.05 ± 0.20**	**3 / 3 — uniform ✓**
G4	0.922	0.416	0.000	0.45 ± 0.46	**2 / 3 — uneven**
G5	0.515	0.000	0.274	0.26 ± 0.26	**2 / 3 — uneven**

Note. ✓ = detected at all three measurement points (uniform distribution); ⚠ = detected at two of three measurement points only (uneven distribution). G3 showed the highest mean phosphorus content and the most consistent detection pattern, indicative of homogeneous oil distribution. G4 and G5 showed intermittent detection with higher variability, consistent with phase-separated, clustered oil distribution.

Table 6. Color stability (ΔE) by group.

Group	n	Mean ΔE	SD	Tukey Group
G1 (Reference)	10	0.00	± 0.00	*
G2	10	1.43	± 0.28	**a**
G3	10	2.38	± 0.28	**b**
G4	10	2.89	± 0.19	**c**
G5	10	4.01	± 0.37	**d**

** G1 = unmodified control; designated as the colour reference baseline (ΔE = 0). Statistical comparison was performed among G2–G5 only, as G1 represents the reference standard against which all modified groups were measured.*

Table 7. One-way ANOVA — color stability (ΔE).

Source	df	F-value	p-value
Between groups	3, 36	140.76	**6.10×10^{-20} ***

Table 8. Tukey HSD pairwise comparisons — color stability (ΔE).

Comparison	Mean Diff.	SE	q-statistic	p-value
G2 vs G3	-0.950	0.0908	10.467	**5.81×10^{-8}**
G2 vs G4	-1.466	0.0908	16.152	**9.53×10^{-13}**
G2 vs G5	-2.584	0.0908	28.469	**4.89×10^{-15}**
G3 vs G4	-0.516	0.0908	5.685	**0.0016**
G3 vs G5	-1.634	0.0908	18.003	**4.55×10^{-14}**
G4 vs G5	-1.118	0.0908	12.318	**1.29×10^{-9}**

Table 9. Compressive strength (MPa) by group.

Group	n	Mean (MPa)	SD	Tukey Group
G3	10	97.10	± 3.75	**a**
G1	10	89.39	± 3.13	**b**
G2	10	80.98	± 4.49	**c**

Group	n	Mean (MPa)	SD	Tukey Group
G4	10	39.22	± 2.61	**d**
G5	10	22.74	± 1.82	**e**

Table 10. One-way ANOVA — compressive strength.

Source	df	F-value	p-value
Between groups	4, 45	999.51	**2.59e-43 ***

Table 11. Tukey HSD pairwise comparisons — compressive strength.

Comparison	Mean Diff.	SE	q-statistic	p-value
G1 vs G2	8.42	1.040	8.09	**7.85e-6**
G1 vs G3	-7.71	1.040	7.41	**3.92e-5**
G1 vs G4	50.17	1.040	48.23	**0.00e+0**
G1 vs G5	66.65	1.040	64.07	**0.00e+0**
G2 vs G3	-16.13	1.040	15.50	**2.69e-13**
G2 vs G4	41.76	1.040	40.14	**0.00e+0**
G2 vs G5	58.24	1.040	55.98	**0.00e+0**
G3 vs G4	57.88	1.040	55.64	**0.00e+0**
G3 vs G5	74.36	1.040	71.48	**0.00e+0**
G4 vs G5	16.48	1.040	15.84	**1.30e-13**

Table 12. Surface microhardness (VHN) by group.

Group	n	Mean (VHN)	SD	Tukey Group
G2	10	73.33	± 2.56	**a**
G3	10	56.29	± 3.83	**b**
G1	10	44.40	± 3.99	**c**
G4	10	37.84	± 2.01	**d**
G5	10	29.75	± 2.00	**e**

Table 13. One-way ANOVA — surface microhardness.

Source	df	F-value	p-value
Between groups	4, 45	320.54	**1.94e-32 ***

Table 14. Tukey HSD pairwise comparisons — surface microhardness.

Comparison	Mean Diff.	SE	q-statistic	p-value
G1 vs G2	-28.93	0.951	30.43	**0.00e+0**
G1 vs G3	-11.89	0.951	12.51	**2.10e-10**
G1 vs G4	6.56	0.951	6.90	**1.30e-4**
G1 vs G5	14.65	0.951	15.41	**3.28e-13**
G2 vs G3	17.04	0.951	17.92	**0.00e+0**
G2 vs G4	35.49	0.951	37.33	**0.00e+0**
G2 vs G5	43.58	0.951	45.84	**0.00e+0**
G3 vs G4	18.45	0.951	19.41	**0.00e+0**
G3 vs G5	26.54	0.951	27.91	**0.00e+0**
G4 vs G5	8.09	0.951	8.51	**2.86e-6**

Table 15. Surface roughness, Ra (µm), by group.

Group	n	Mean (µm)	SD	Tukey Group
G2	10	0.49	± 0.05	**a**
G3	10	0.50	± 0.06	**a**
G4	10	0.70	± 0.08	**b**
G1	10	0.81	± 0.07	**b**
G5	10	1.06	± 0.17	**c**

Table 16. One-way ANOVA — surface roughness.

Source	df	F-value	p-value
Between groups	4, 45	60.39	**1.62e-17 ***

Table 17. Tukey HSD pairwise comparisons — surface roughness.

Comparison	Mean Diff.	SE	q-statistic	p-value
G1 vs G2	0.33	0.031	10.63	**1.73e-8**
G1 vs G3	0.32	0.031	10.37	**3.22e-8**
G1 vs G4	0.12	0.031	3.75	0.0778
G1 vs G5	-0.24	0.031	7.96	**1.07e-5**
G2 vs G3	-0.01	0.031	0.26	0.9997
G2 vs G4	-0.21	0.031	6.88	**1.35e-4**

Comparison	Mean Diff.	SE	q-statistic	p-value
G2 vs G5	-0.57	0.031	18.59	**0.00e+0**
G3 vs G4	-0.20	0.031	6.62	**2.46e-4**
G3 vs G5	-0.56	0.031	18.33	**0.00e+0**
G4 vs G5	-0.36	0.031	11.71	**1.35e-9**

Figure Captions

Figure 1. Stacked Fourier-transform infrared (FTIR) spectra of garden cress oil (GCO), Gum Arabic (GA) powder, and the five experimental glass ionomer cement groups (G1–G5) across the wavenumber range 400–4000 cm^{-1}. Spectra are baseline-corrected and normalised. Key absorption bands are labelled: O–H stretching (3343–3396 cm^{-1}), aliphatic C–H stretching (~2922 cm^{-1}), carbonyl/carboxylate region (1581–1634 cm^{-1}), C–H bending (~1456 cm^{-1}), and Si–O–Si/C–O band (1024–1038 cm^{-1}). The ester carbonyl band of pure GCO at 1746.4 cm^{-1} is diagnostic for triglyceride content. G3 (GIC + 0.5 wt.% Gum Arabic + 0.5 vol.% GCO) exhibits the deepest carbonyl/carboxylate absorption (minimum transmittance = 0.746) of all cement groups, indicating maximum matrix chemical interaction at this concentration. ATR-FTIR spectroscopy.

Figure 2. Representative scanning electron micrographs of the polished surfaces of the five experimental groups at ×2,000 magnification. (A) G1: unmodified conventional glass ionomer cement (control), demonstrating moderately compact surface morphology with scattered glass particles and localized surface depressions. (B) G2: GIC modified with 0.5 wt.% Gum Arabic alone, showing a smoother and more homogeneous surface with improved matrix continuity compared to the control. (C) G3: GIC modified with Gum Arabic and 0.5 vol.% garden cress oil, exhibiting a compact and uniform surface without evidence of discrete oil phase separation.

(D) G4: GIC modified with Gum Arabic and 1.0 vol.% garden cress oil, demonstrating progressive surface disruption with visible cracking and delamination zones. (E) G5: GIC modified with Gum Arabic and 1.5 vol.% garden cress oil, showing the most severely disrupted surface morphology with extensive cracking, matrix delamination, and rounded globular surface features consistent with surface-localized oil accumulation.

Figure 3. Representative scanning electron micrographs of the polished surfaces of the five experimental groups at ×5000 and ×10000 magnifications. (A) G1: unmodified conventional glass ionomer cement (control), demonstrating a smooth, compact polyacrylate matrix with sparsely distributed glass particle remnants serving as the morphological baseline. (B) G2: GIC modified with 0.5 wt.% Gum Arabic alone, revealing well-defined surface features consistent with surface enrichment of the hydrophilic Gum Arabic carrier during the aqueous cement setting phase. (C) G3: GIC modified with Gum Arabic and 0.5 vol.% garden cress oil, showing a compact matrix texture without identifiable discrete oil droplet features at the surface, supporting homogeneous oil incorporation at this concentration. (D) G4: GIC modified with Gum Arabic and 1.0 vol.% garden cress oil, demonstrating surface cracking alongside early-stage rounded globular features suggestive of incompletely stabilized oil droplets, indicating partial emulsification failure at this concentration. (E) G5: GIC modified with Gum Arabic and 1.5 vol.% garden cress oil, exhibiting densely distributed, clearly defined spherical features consistent with surface-accumulated, non-incorporated oil droplets, providing morphological evidence that the emulsification capacity of 0.5 wt.% Gum Arabic was exceeded at 1.5 vol.% oil, contributing to the severe matrix disruption and lowest mechanical property values recorded across all experimental groups.

Figure 4. (A) Stacked EDX X-ray energy spectra for the five experimental groups (G1–G5), presented as normalised intensity (0–1 relative to maximum) across the energy range 0.1–7.5 keV. Bold line = mean spectrum (n = 3 measurement points per group); faint lines = individual measurement points. Red bold annotation = N Kα (0.392 keV): nitrogen derived from the arabinogalactan-protein complex of Gum Arabic; instrument-confirmed absent in G1, consistently present in G2–G5. Teal bold annotation = P Kα (2.013 keV): phosphorus from the phospholipid fraction of Lepidium sativum fixed oil; confirmed absent in G1 and G2, uniformly detected at all three measurement points in G3 (homogeneous oil distribution), and variably detected in G4 and G5 (asterisk; instrument-identified at all points but quantification yielded zero at one point per group, consistent with phase-separated oil distribution). (B) Mean

spectrum overlay for all five groups: full energy ranges 0.1–7.5 keV (left) and expanded diagnostic region 0.25–2.3 keV (right), with N Kα (red dashed) and P Kα (teal dashed) positions indicated, confirming their progressive appearance across the concentration series. (C) Quantitative grouped bar chart of mean elemental weight percent (Wt%) for all detected elements (C, N, O, F, Al, Si, Ca, P) across the five groups; inset shows N and P alone to highlight the diagnostic markers. Data: n = 3 measurement points per group; see Tables 4 and 5 for individual point values. EDX at 20 kV; Thermo Fisher Scientific Pathfinder system, EDS1 detector (Si-drift crystal, 30 mm^2).

Figure 5. Mechanical and surface property outcomes of the five experimental glass ionomer cement groups. (A) Compressive strength (MPa); (B) Vickers surface microhardness (VHN); (C) Surface roughness expressed as mean arithmetic roughness (Ra, μm). All values represent means of n = 10 specimens per group. Error bars represent ± standard deviation. Different letters above bars denote statistically significant differences between groups (one-way ANOVA with Tukey HSD post-hoc test; $\alpha = 0.05$). Groups sharing the same letter are not significantly different from each other. G1: unmodified conventional glass ionomer cement (control); G2: GIC supplemented with 0.5 wt.% Gum Arabic alone (no oil); G3: GIC supplemented with Gum Arabic and 0.5 vol.% garden cress oil (Lepidium sativum); G4: GIC supplemented with Gum Arabic and 1.0 vol.% garden cress oil; G5: GIC supplemented with Gum Arabic and 1.5 vol.% garden cress oil. Note the differential ranking between compressive strength (G3 > G1 > G2 > G4 > G5) and surface microhardness (G2 > G3 > G1 > G4 > G5), reflecting the distinct surface-versus-bulk partitioning behaviour of Gum Arabic during the aqueous cement setting phase. G3 achieved the most favorable overall mechanical profile across all three outcome measures.

Declarations

Ethics Statement

This research did not involve any human subjects or animal specimens, and it was performed in accordance with the institutional regulations.

Consent for publication Not applicable.

Availability of supporting data

The data that support the findings of this study are available from the corresponding author upon reasonable request.

Competing interest

The authors have no competing interests to declare that are relevant to the content of this article.

Funding

- The authors did not receive financial support from any organization for the submitted work.
- All authors certify that they have no affiliations with or involvement in any organization or entity with any financial interest or non-financial interest in the subject matter or materials discussed in this manuscript.

Authors Contributions

Conceptualization, study design, data collection, data interpretation, measurement of compressive strength, surface microhardness, surface roughness, spectrophotometric assessment, scanning electron microscopy, FTIR, EDX, statistical analysis, writing and submission of the manuscript were done by NSA.

Acknowledgements

Not Applicable

Using AI tools

The author used AI tools exclusively for language editing and stylistic improvements in the manuscript. The tool was not employed for study design, data collection, measurements, statistical analysis, or interpretation of results. All scientific content and conclusions were developed and verified by the author.

Comparative FTIR Spectra: Garden Cress Oil, Gum Arabic, and Modified Conventional GIC

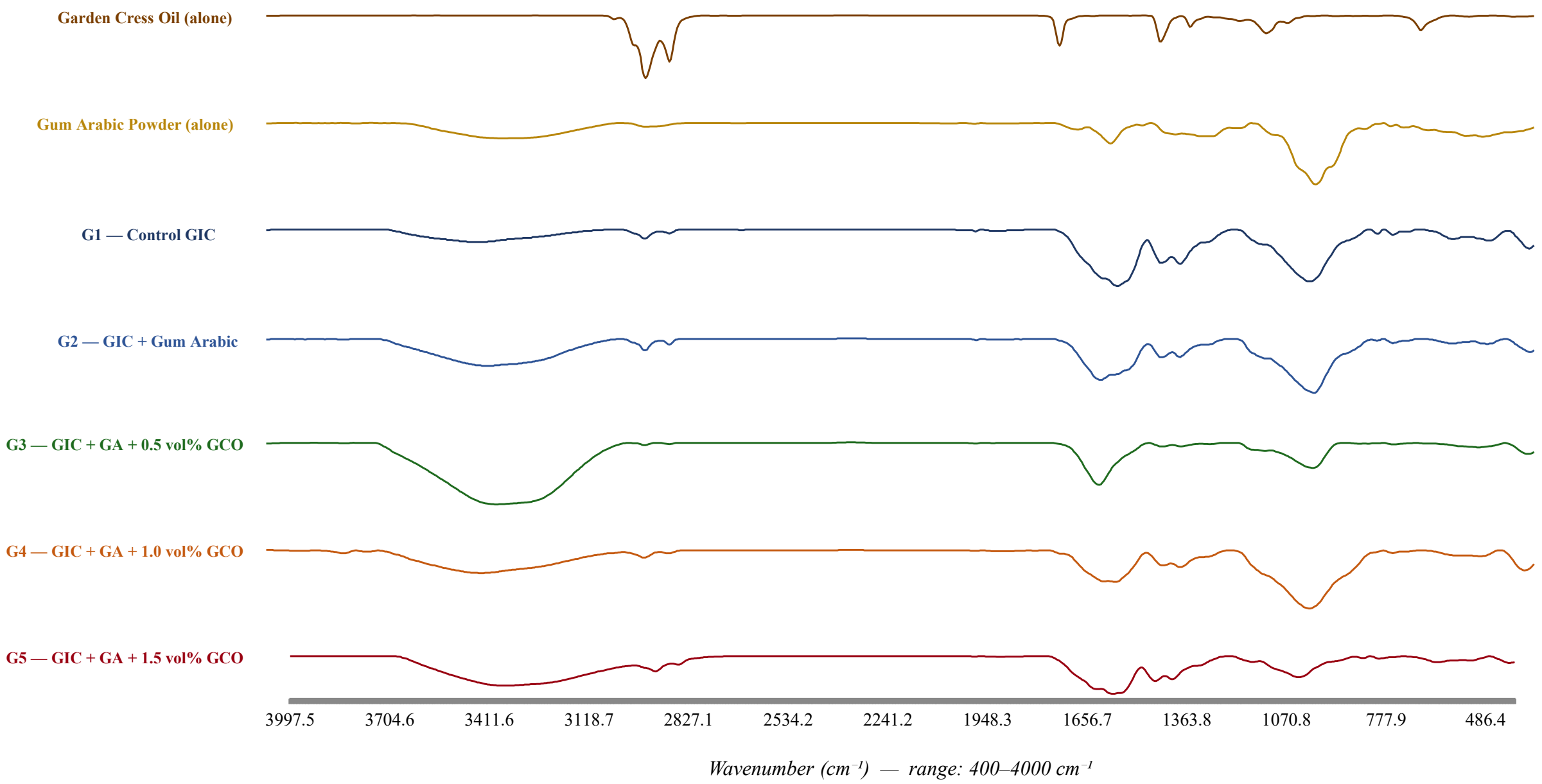

Table 1. Verified FTIR Peak Positions (cm^{-1}) — Reference Components and Experimental Groups

Spectral Region	GCO	GA	G1	G2	G3	G4	G5	Tentative Assignment
O–H stretch	—	3309.2	3396.0	3367.5	3343.4	3387.4	3363.3	Hydroxyl/adsorbed water; progressive red-shift G1→G3 indicates increased H-bonding
=C–H stretch (unsaturation)	**3009.2**	—	—	—	—	—	—	cis-Unsaturated fatty acid marker — unique to garden cress oil
Aliphatic C–H stretch	2921.0	2918.2	2922.4	2922.4	2922.4	2925.3	2923.8	CH_2 asymmetric stretch — strongest in pure oil
Ester C=O stretch	**1746.4**	—	—	—	—	—	—	Triglyceride ester carbonyl — unique to oil; not resolved in composite spectra (see Note)
Carbonyl/carboxylate region	—	1601.3	1582.8	1629.7	**1634.0**	1589.9	1581.4	Amide I/carboxylate (GA); polyacrylate C=O/COO^- (GIC); strongest in G3
C–H bending	1459.1	—	1456.2	1456.2	1456.2	—	1454.8	CH_2/CH_3 bending
COO^- symmetric stretch	—	—	1405.0	1405.0	1402.2	1403.6	1405.0	Polyacrylate carboxylate symmetric stretch — consistent across GIC groups
Si–O–Si / C–O	1025.3	1018.2	1036.7	1023.9	1026.8	1038.1	1033.9	Glass Si–O–Si and Gum Arabic C–O–C stretch (overlapping)
Min. transmittance	0.546	0.653	0.918	0.914	**0.746**	0.865	0.894	Overall absorption intensity — G3 strongest among cement groups

Note. GCO = garden cress oil (alone); GA = Gum Arabic powder (alone). The ester carbonyl band at 1746.4 cm^{-1}, clearly resolved in the pure garden cress oil spectrum, was not similarly resolved as a discrete feature in any of the five composite cement groups (G1–G5), likely reflecting the low oil fraction within the set cement and spectral overlap with the dominant, more intense native GIC carbonyl absorption in the same region. Specimen G3 exhibited the most intense overall absorption (minimum transmittance = 0.746) and the most clearly resolved carbonyl band (1634.0 cm^{-1}) among all five cement groups.

SE Micrographs at X 2000 for all experimental groups

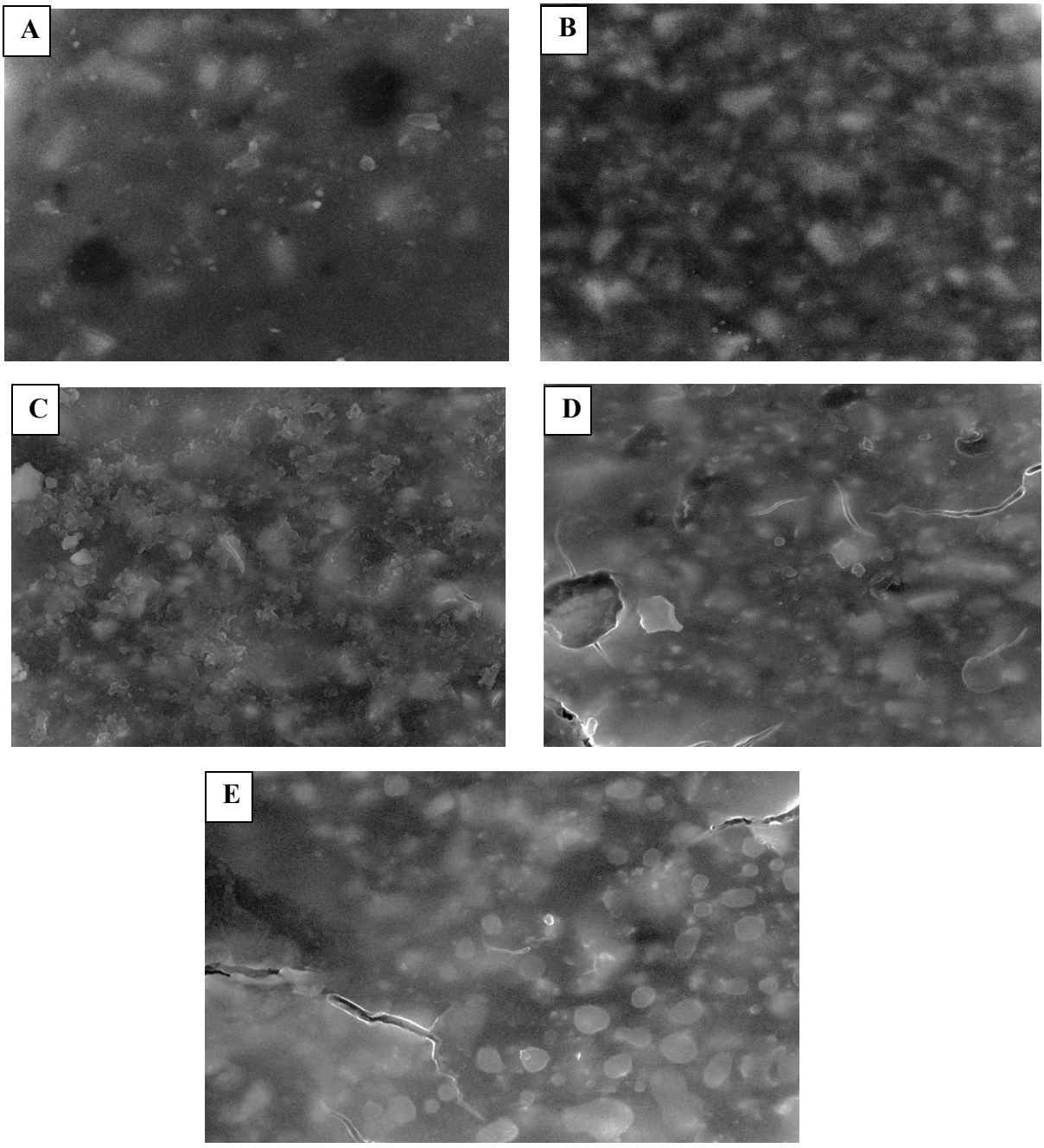

Magnification X5000

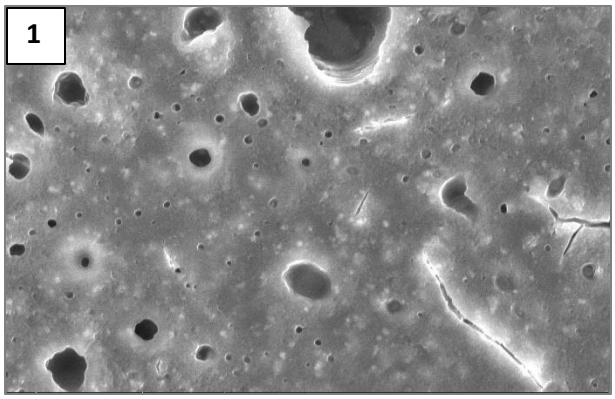

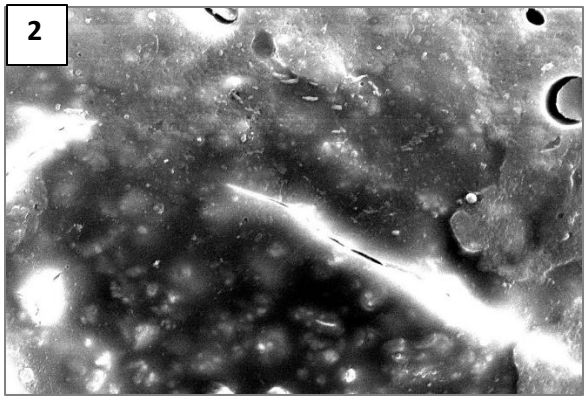

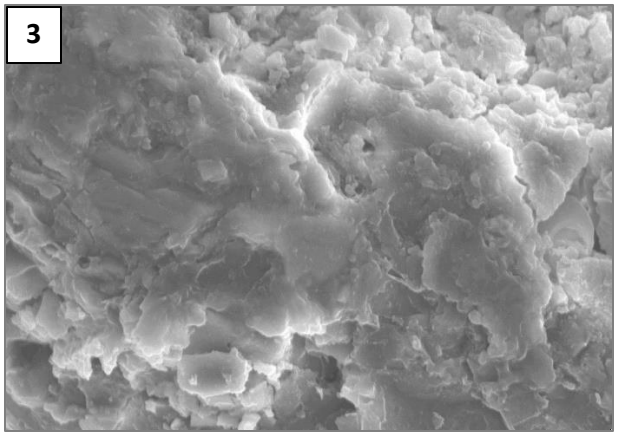

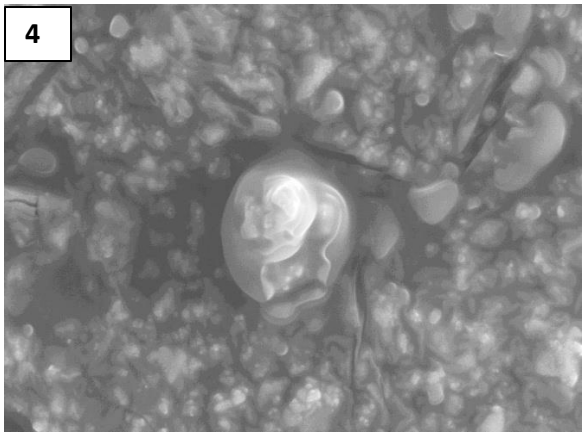

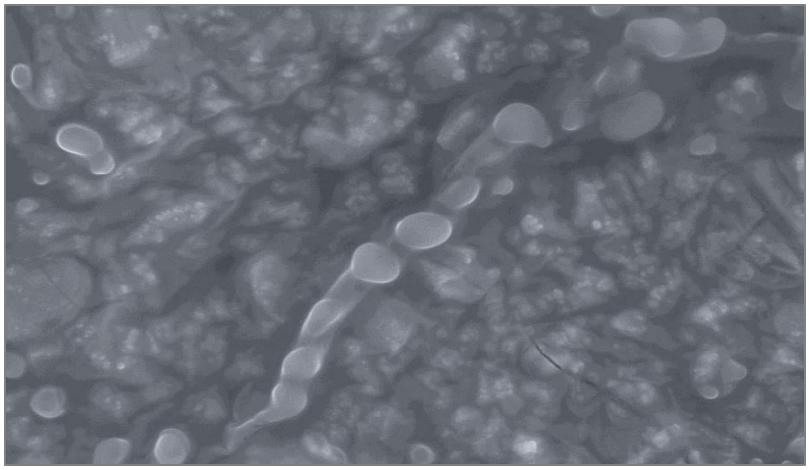

Magnification X10000

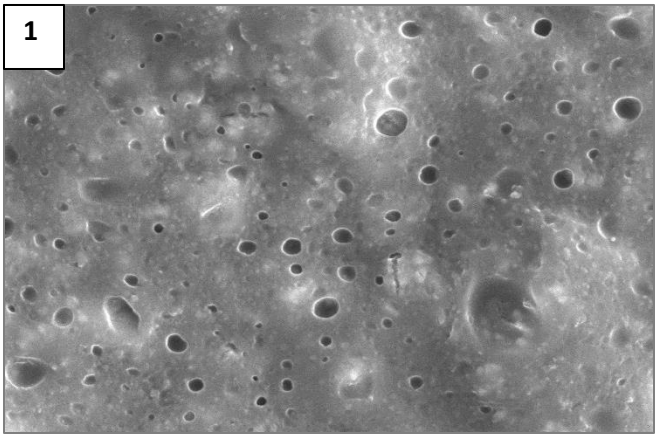

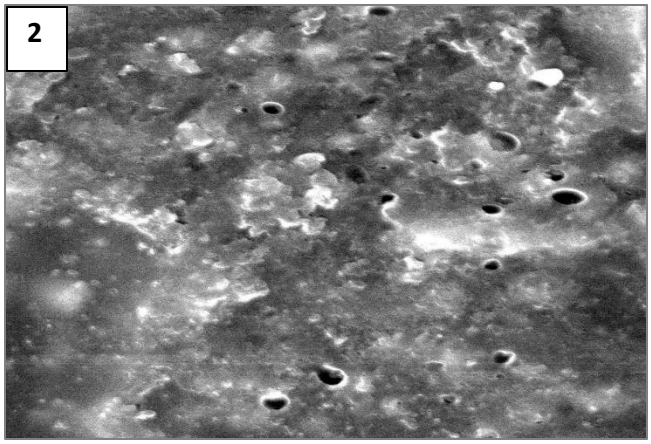

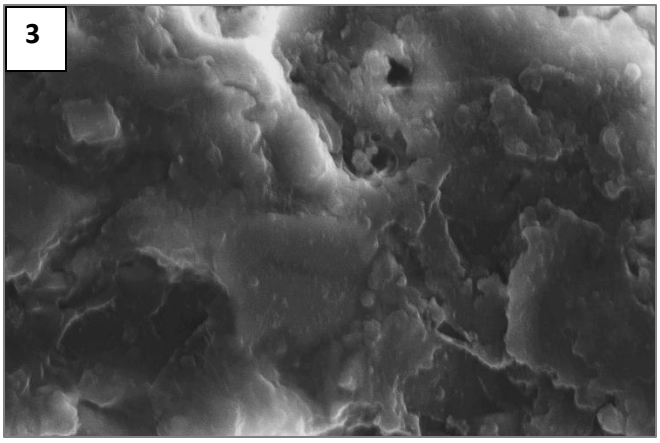

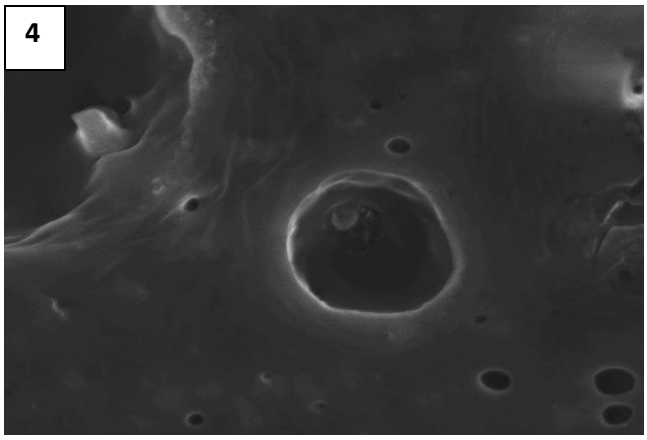

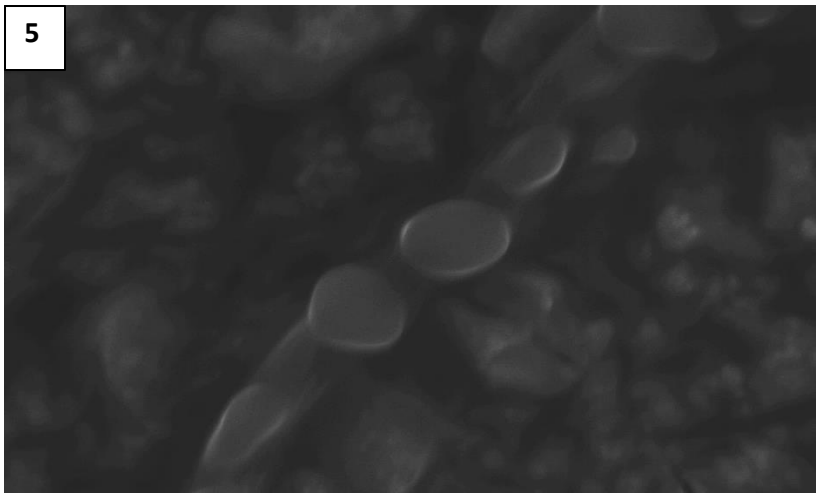

Figure 4A. EDX X-ray Energy Spectra — Five Experimental Groups (Stacked)

*Spectra normalised to maximum intensity. Bold line = mean (n = 3); faint lines = individual measurement points. Red bold = N Kα (0.392 keV, Gum Arabic protein marker; absent in G1). Teal bold = P Kα (2.013 keV, Garden Cress Oil marker; absent in G1–G2; uniform in G3; variable in G4–G5). * = instrument-detected but quantification variable at one point.*

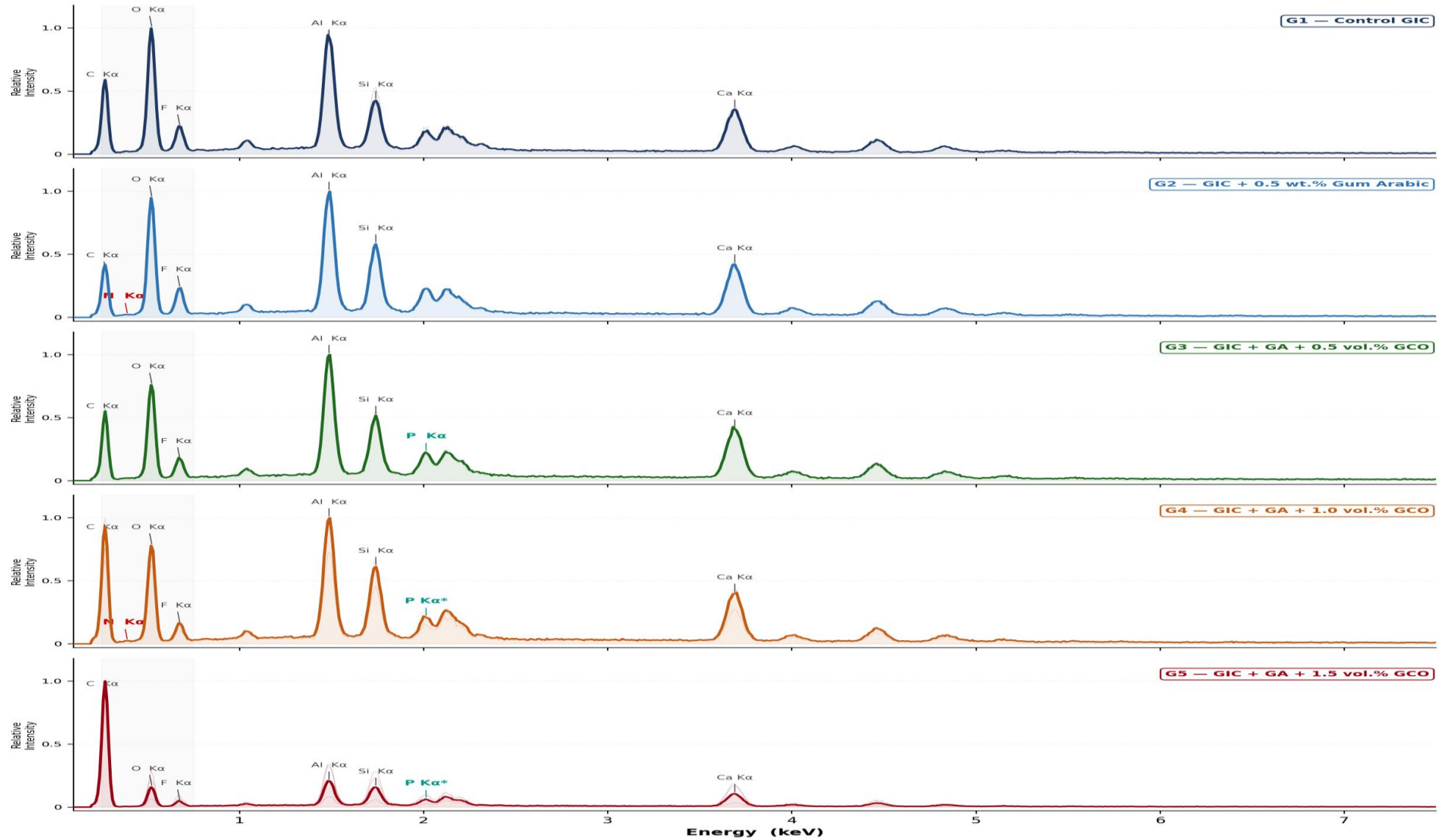

Figure 4B. EDX Mean Spectrum Overlay — All Groups (Full Range & Diagnostic Region)

(Left) Full spectrum overlay 0.1–7.5 keV. (Right) Expanded diagnostic region 0.25–2.3 keV showing progressive appearance of N Kα (red dashed) from G2 onwards and P Kα (teal dashed) from G3 onwards. Note flat baseline at N Kα position in G1 and at P Kα position in G1 and G2.

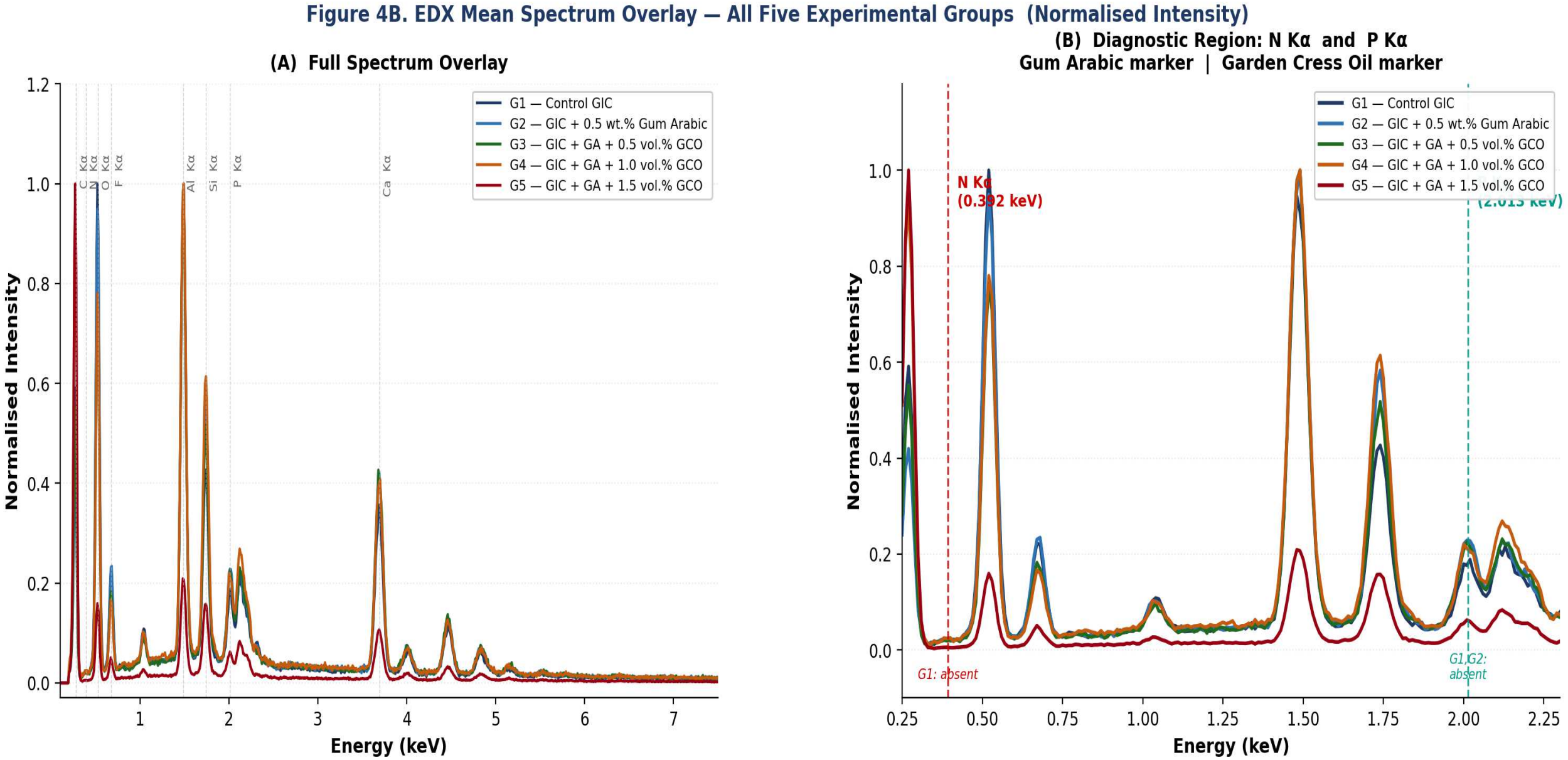

Figure 4C. EDX Elemental Composition — Quantitative Bar Chart (Mean Wt%)

Mean elemental weight percent (Wt%) ± SD at three measurement points per group. G1 = unmodified control; G2 = GIC + Gum Arabic; G3–G5 = GIC + Gum Arabic + 0.5, 1.0, 1.5 vol.% GCO. N and P absent in G1 (no Gum Arabic, no oil). P absent in G2 (no oil). See Tables 4 and 5 for raw values.

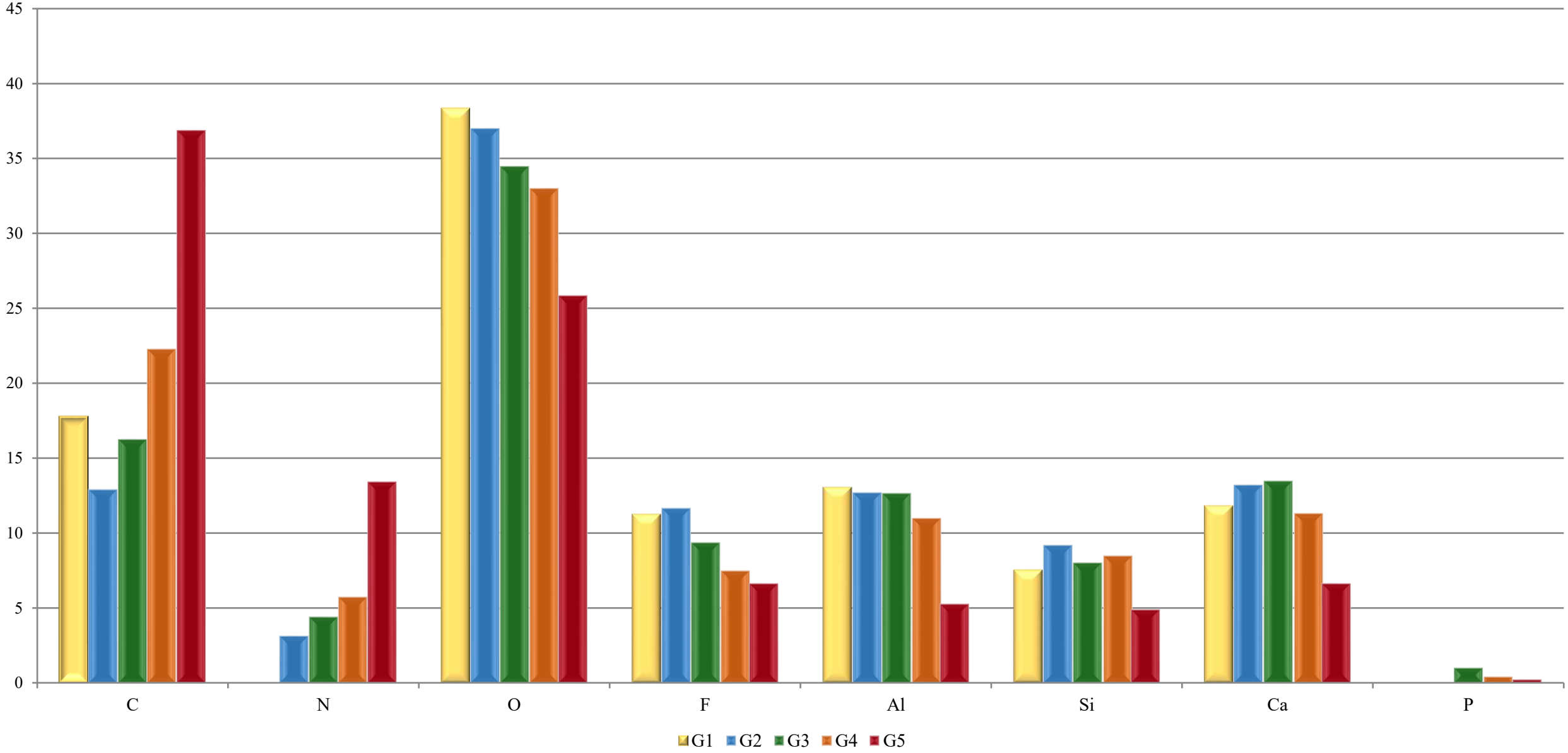

Figure 4C (inset). Diagnostic Markers Only: N Kα and P Kα Weight%

Left: Nitrogen (N Wt%) — Gum Arabic protein marker, absent in G1, increasing G2→G5. Right: Phosphorus (P Wt%) — Garden Cress Oil marker, absent in G1 and G2, highest and most consistent in G3 (uniform oil distribution), lower and variable in G4–G5 (phase-separated oil distribution). See Table 5 for individual point values.

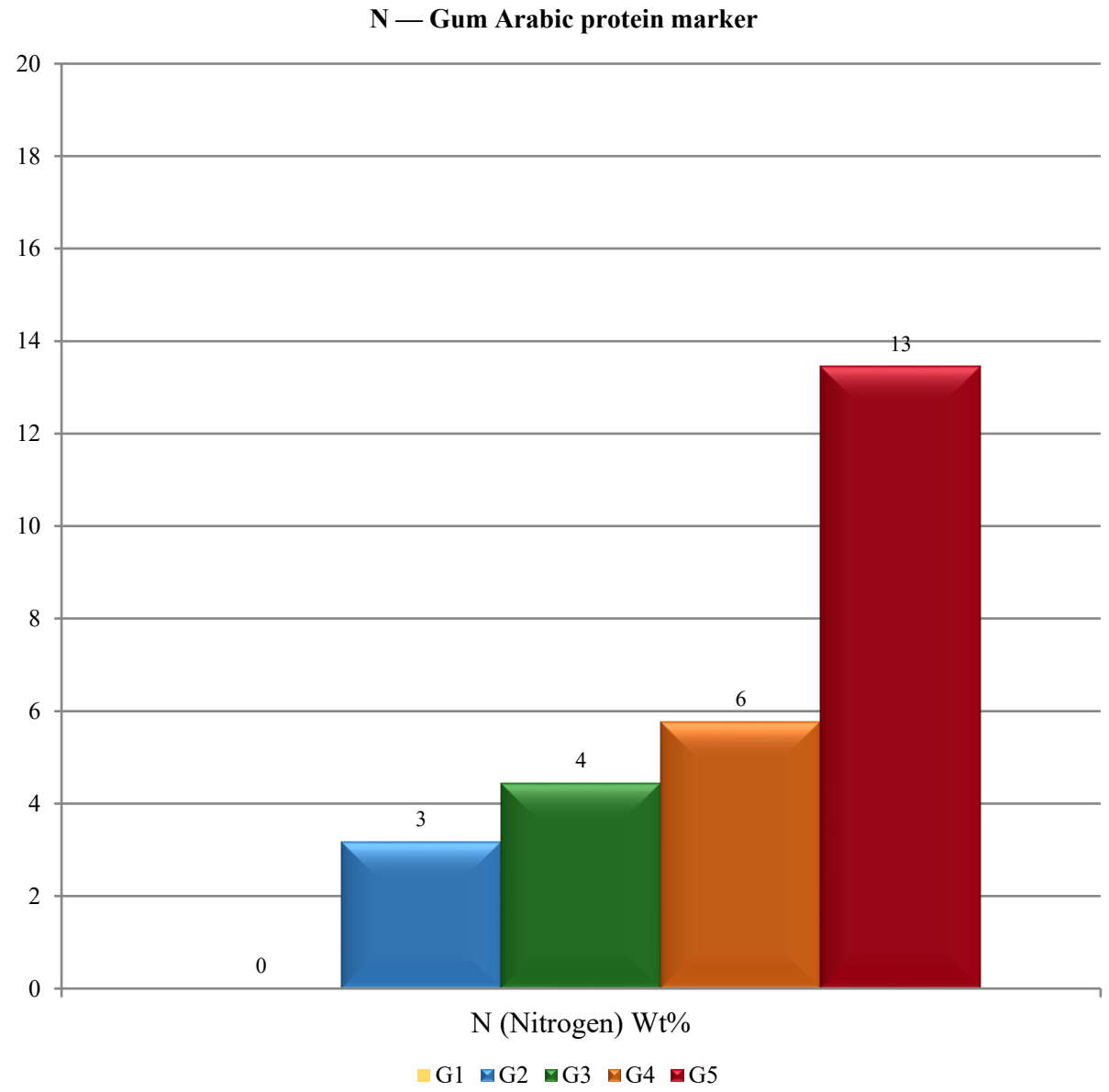

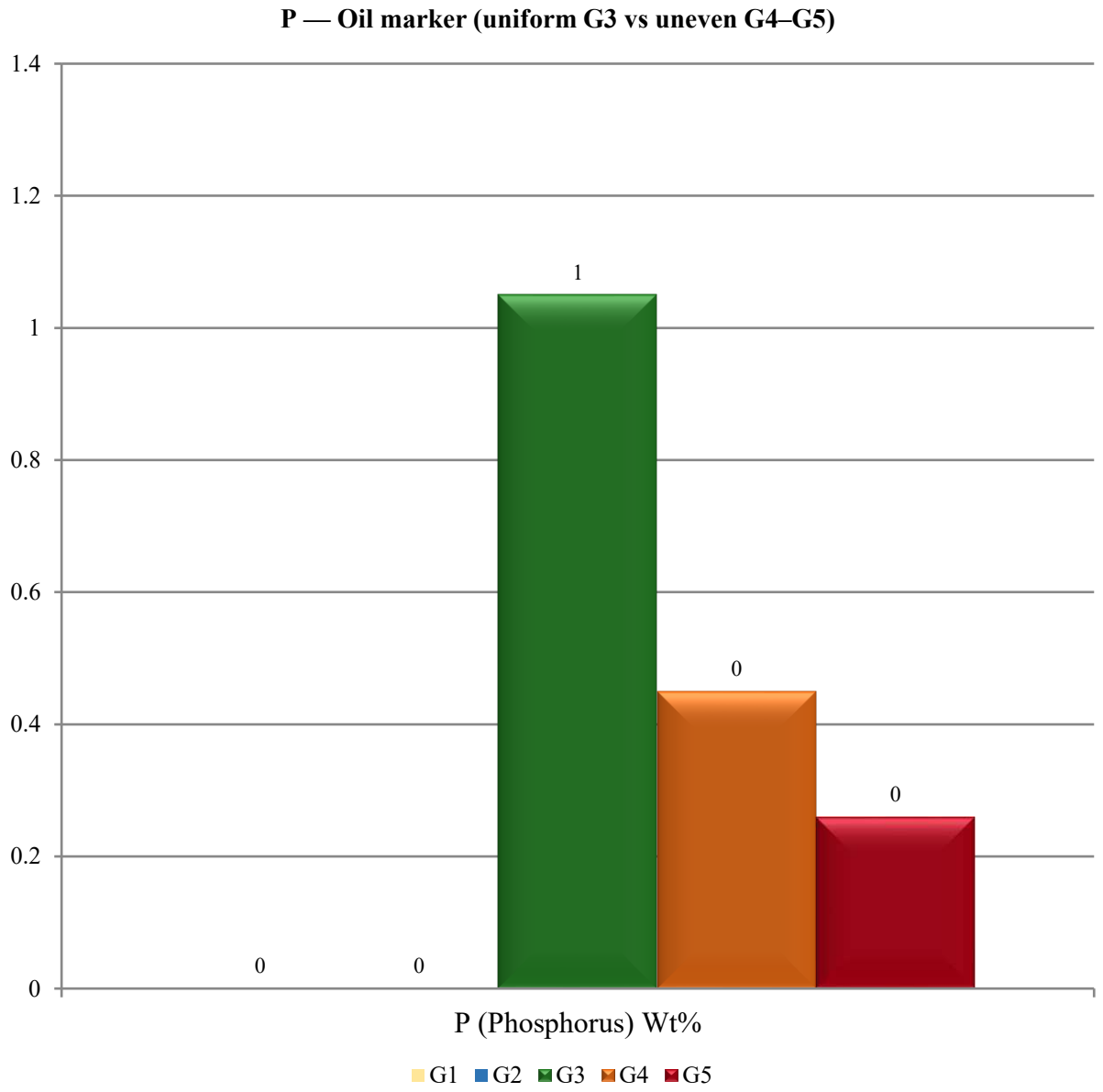

Figure 5. Mechanical and surface property outcomes across the five experimental groups